SYNERGISM OF Rn-222 REDUCTION EMANATION WITH DIFFERENT TYPE OF COATINGS FROM RED BRICKS

by

ASMAT BINTI ZAHARIMAN

A report submitted in fulfillment of the requirements for the degree of Bachelor of Applied Science (Materials Technology) with Honours

FACULTY OF EARTH SCIENCE
UNIVERSITI MALAYSIA KELANTAN

2017

DECLARATION

I declare that this thesis entitled “Synergism of Rn-222 Reduction Emanation with Different Type of Coatings From Red Bricks”is the result of my own research except as cited in the references. The thesis has not been accepted for any degree and is not concurrently submitted in candidature of any other degree.

Signature : _____

Name : ASMAT BINTI ZAHARIMAN

Date : _____

ACKNOWLEDGEMENT

Alhamdulillah praise to Allah S.W.T for his blessing and guidance in giving me the ability and strength in finishing my final year project and my thesis

First and foremost, I would like to express my gratitude towards the Faculty of Earth Science, Universiti Malaysia Kelantan for giving the opportunity of conducting the research for my Final Year Project.

I would like to express my gratitude to my supervisor, Dr. Mohammad Khairul Azhar Abdul Razab, for his encouragement in pursuing this research, for the shared information and knowledge related to the topic and for the motivation which has driven me to do well in completing this thesis. Special thanks to all of my final year project partners, Mohd Ibrohim bin Abdullah for helping each other in completing this project and my close friend Ahmad Syakir bin Ismail@Ramli for the knowledge and guidance given to me on how to deal with related software, thus completing this thesis. A special gratitude goes to the lab assistants, mainly En.Rohanif for the guidance in dealing with the equipment used in this project.

I also would like to express my gratitude to both of my parents for their support and passionate encouragement in which have made it possible for me to complete this project. Their moral support has given me the strength to finish this project according to the given duration.

Thanks to all of my friends who always share their knowledge and information in completing this thesis. Some of them have the interest to my project and it is a great motivation for me throughout the progress of the research. Last but not least, thanks to all for supporting this research directly or indirectly.

Synergism of Rn-222 Reduction Emanation with Different Type of Coatings from Red Bricks

ABSTRACT

Radon is one of the radiation sources which occurs naturally in the environment. It is a form of radioactive gas and one of the contributors for lung cancer besides smoking due to the emission of alpha particles. Radon (Rn-222) can be found in common building materials such as the red bricks and it is derived from the series decay process of Uranium (U-238). It is produced from the combination of sand, cement, and possibly clay to form a bulk of bricks. These aggregates are also consisting of Rn-222 concentration. People in Malaysia do not realize the existence of Rn-222 emanates from red bricks. Rn-222 emanates from the red bricks through the porosity and also the cracking line along the bricks. In order to prevent emanation of α-particles Rn-222 progenies from red bricks, a layer of plaster was applied. This plaster was then coated with selected coating which are Jotun, Nippon Paint, and Dulux. Radon Sentinel 1030 monitor was used to measure the concentration of Rn-222 that emanates from the brick before and after coated with different types of coating materials. The concentration of Rn-222 had decreased after being coated with coating materials. However, the concentration of Rn-222 in the layer applied with only plaster is in the range of -0.6pCi/L to -0.9pCi/L. The concentration of layer applied with plaster coated with Jotun was in between -0.8pCi/L to -1.0pCi/L whereas the plaster coated with Nippon was from -0.3pCi/L to -0.9pCi/L and the layer coated with Dulux was in between -0.7pCi/L to -0.8pCi/L.

Synergism Pengurangan keluar pergi Rn-222 dengan jenis salutan yang berbeza dari bata merah

ABSTRAK

Radon adalah salah satu jenis sumber radiasi dan ia berlaku secara semula jadi dalam persekitaran. Ia adalah salah satu gas radioaktif dan salah satu penyumbang untuk penyakit kanser paru-paru selepas merokok disebabkan oleh pelepasan zarah alfa. Radon (Rn-222) boleh didapati dalam bahan-bahan bangunan biasa seperti batu bata merah dan ia berasal daripada proses siri pereputan Uranium (U-238). Ia adalah bentuk dari gabungan pasir, simen, dan mungkin tanah liat untuk membentuk sebahagian besar daripada batu bata.Agregat ini juga mengandungi kepekatan Rn-222secara semulajadi. Masyarakat di Malaysia tidak menyedari kewujudan Rn-222 yang berasal dari bata merah. Rn-222 akan keluar melalui liang dan juga garisan keretakan yang terdapat di dalam struktur bata. Untuk mengelakkan emanasi daripada α-zarah Rn-222 progeni daripada batu bata merah, lapisan plaster telah digunakan. Plaster ini kemudian disalut dengan salutan terpilih iaitu Jotun, Nippon Paint, dan Dulux. Radon Sentinel 1030 monitor digunakan untuk mengukur kepekatan Rn-222 dari bata sebelum dan selepas disalut dengan bahan salutan yang dipilih. Kepekatan Rn-222 berkurang selepas disalut dengan bahan salutan. Kepekatan Rn-222 yang keluar dari bata dengan hanya menggunakan plaster adalah diantara -0.6pCi / L ke -0.9pCi / L. Kepekatan Rn-222 yang keluar dari bata dengan menggunakan plaster disalut dengan Jotun adalah diantara -0.8pCi / L ke -1.0pCi / L manakala plaster disalut dengan Nippon adalah dari -0.3pCi / L ke -0.9pCi / L dan lapisan disalut dengan Dulux adalah antara -0.7pCi / L ke -0.8pCi / L.

TABLE OF CONTENT

LIST OF TABLE

LIST OF FIGURES

LIST OF ABBREVIATIONS

GBFS	Granulated Blasted Furnace Slag
pCi	Picocuries
Rn	Radon
ASTM	American Society for Testing and Materials
BG	Borogypsum
UV	Ultraviolet
NORM	Naturally Occurring Radioactive Materials
TBC	Thermal Barrier Coating
EPA	Environmental Protection Agency

LIST OF SYMBOLS

η	Viscosity
ρ	Density
g	Standard Gravity
r	Radius
v	Velocity

CHAPTER 1

INTRODUCTION

1.1 Background of Study

Radiation is random and may be found anywhere in our life, especially Radon (Rn-222) gas which has naturally existed in the air surrounding our environment. It is one of the radioactive gases originated from the earth's crust. Rn-222 can easily penetrate the building materials through the porosity of material due to its nature of being one of the inert or noble gases in the group of eighteen in the periodic table. As a noble gas, Rn-222 is characterized naturally as odourless, colourless, tasteless and invisible to our sense.

Rn-222 can be found naturally in the building materials used like cement and stone. The porosity of the material used tends to make an easy route for Rn-222 to emanate towards the surrounding. According to the inertness of Rn-222, it will move through the building materials and will be inhaled by the people inside the building. The inhalation of Rn-222 will cause severe disease to human, for example lung cancer.

Due to this reason, the research is conducted to investigate the amount of radon emanating from the building materials which is the red brick. The concentration of Rn-222 in the red bricks is one of the maximum concentrations because it consists of natural radioactive nuclides. Usually, natural radionuclides that are embedded in the soil are originated from uranium (^{238}U) and thorium (^{232}Th). Red brick which is formed from the soil is inevitable and contain radionuclides, which is the main source of radiation.

The amount of radon in red brick is considerably high due to the high porosity in the whole structure of the materials. Thus, the Rn-222 is easily emanated towards the building environment. Since Rn-222 has a short half-life span, it easily emanates from the wall and floors of buildings in high exposure with poor ventilation system (Saad et al., 2010; Singh et al., 2005).

1.2 Problem Statement

The people or community rarely concern about the Rn-222 effects among them. The red brick is widely used in building construction without knowing the presence of high radioactivity in the materials used. In order to reduce the emanation of radon exhale from red brick, this research will be conducted by applying different types and composition from selected coating system. By using the proper type of paint and applying it on the emanating media, radon exhalation from the red brick or other materials can be reduced. Thus, this research is conducted to make the community realize and create awareness about the building materials that will be used in constructing a building or houses in the future.

1.3 Research Objective

This research is conducted to achieve the following objectives:

a) To measure the amount of Rn-222 concentration level from the red brick.

b) To determine the effect of different types of coatings in Rn-222 emanations from red brick.

1.4 Expected Outcome

Throughout this research, thickness and porosity of coating material, which is painted, plays an important role in preventing the emanation of radon. The higher the thickness of the paint coating the lower the porosity level resulting in the lower amount of radon emanation towards the surrounding.

1.5 Scope of Study

This study will be conducted in the Perspex prototype room covered by plastic modelling at the edge that will prevent the air from entering the room and act as an intruder towards the measurement concentration of materials in that room. In addition, it is used to maintain the humidity, ventilation, temperature and pressure surrounding that will affect the reading of radon emanation from materials.

The red brick was used as the research sample to measure the amount of radon. This is due to the red brick's preference as one of the materials for local building. Thus, different brands of paint which are Jotun, Dulux, and Nippon Paint will be used as they consist of different composition and porosity. The different in porosity of coating agent will result in different emanation rate of Radon concentration.

CHAPTER 2

LITERATURE REVIEW

2.1 Radioactive Materials

The natural radioactive in building materials is the causes of internal and external radiation occurrence with small amount of radionuclide. The main primordial radioactive materials which occur naturally before the formation of solar system is ^{238}U, ^{232}Th and ^{40}K. The formation of stable radon whether for the radon-220 or radon-222 is from the decay chain of ^{238}U and ^{232}Th.

The existence of radon will cause two types of radiation exposure which are external exposure and internal exposure. For the external exposure, it is caused by the emission of gamma radionuclide in the series of uranium decay chain segment in which started with the radium ^{226}Ra. The external radiation is exposed in the surrounding of a construction environment such as the wall and so on.

The internal exposure in human body is caused by the natural radionuclide in food, water and soil. It can also occur due to the inhalation of radon-220 from the decay chain of Thoron. The concentration of radon daughter is the important parameter in monitoring internal radiation exposure by inhalation (Buonanno et al., 2011).

2.1.1 Radioactive Decay Series

Decay is a splitting process of atom naturally when the certain elements have unstable nuclei. The decay of an atom will form a different isotope either the same element or new element. In order to be a more stable isotope, the element will decay

in multiple times and go through a series of alpha or beta particle. As shown in Figure 2.1, Uranium and their half-life will undergo decay in order to form a stable nuclide.

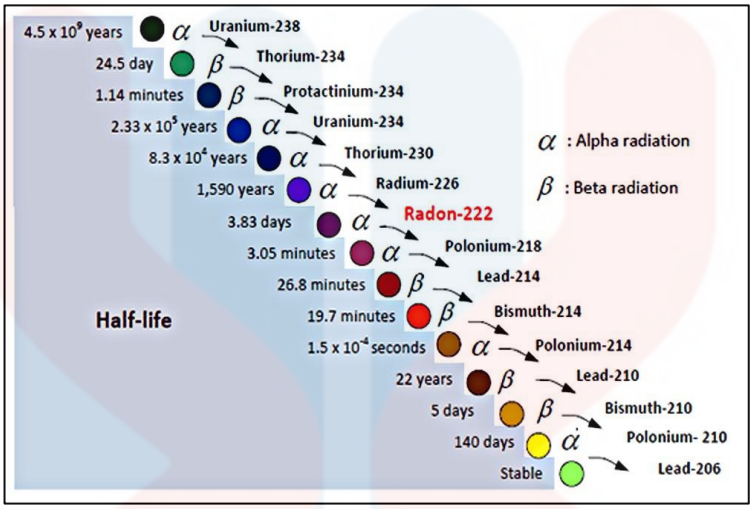

Figure 2.1: The decay chain of Uranium and their half-life (Gosnell & Wong, 2014)

2.1.2 Radon (Rn-222)

Radon-222 is one of the noble radioactive inert gas coming from disintegration of ^{226}Ra and part of decay ^{238} U chain. Radon-222 is characterized as odourless, tasteless and chemically inert and only can be measured with special equipment. It is naturally produced in soils and rock from the earth crust. Figure 2.2 shows the route of the Radon-222 from the wall of brick as they may emit from the porosity of the brick. After the decays of radium ^{226}Ra, radon-222 will leave the soil grain by α-recoil process and move to the atmosphere (Abdallah et al., 2007; Somlai et al., 2007; Tabar & Yakut, 2013).

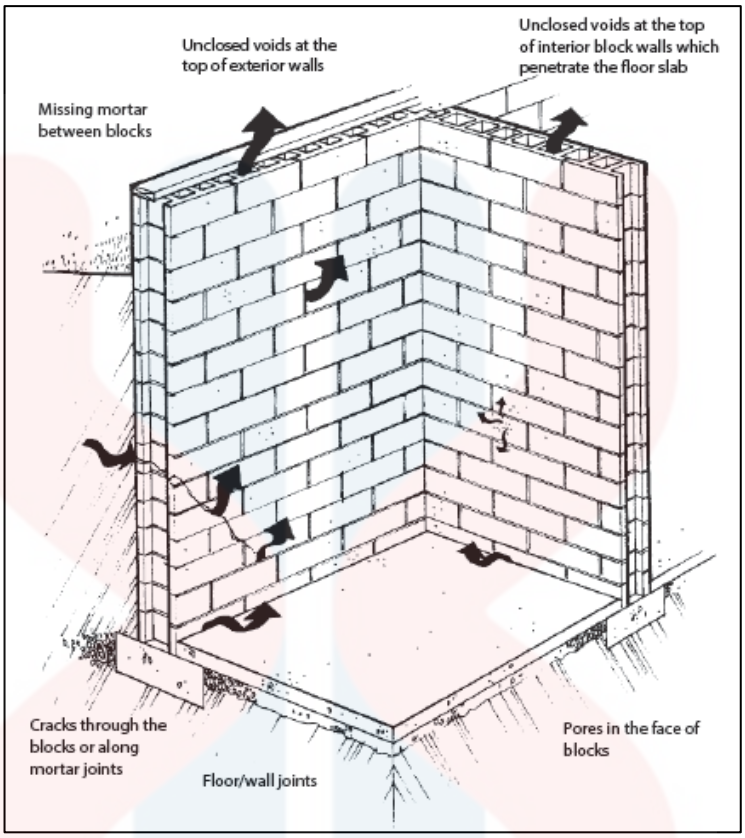

Figure 2.2: Route of Rn-222 from wall of brick (Hay, 2015)

When the radium atom moves near to the surface of grain, the alpha recoil will send the radon atom deeper into the grain as the direction of recoil is towards the grain core. The newly formed of radon will leave the mineral and enter the pore space between the grain in the rocks or other source if the recoil of some radon move near the surface of a grain. The process of alpha recoil is important as the radon will dislodge from the edge of mineral soil matrix and will enable it to penetrate pore space between the soil grains.

Besides, turbidity and concentration of ^{222}Rn in ground water have a strong relationship. The observation shows that its concentration increases at higher level of turbidity (Aleissa et al., 2013). Thus, the higher the turbidity, the concentration of ^{222}Rn would be higher.

2.1.3 Health Effect of Radon

Since the radon emanates towards surrounding from breathing air, it gives high risk of health of radon ingestion. Radon that is exposed in the air is dangerous due to the successively decay of their daughter such as ^{214}Bi with β-rays and γ-rays. The inhalation of the gas and its decays products into the respiratory system will be absorbed by the lung tissue and increases the lung cancer and other health problems risks (Wang *et al*., 2002).

The adverse health effect of radon exposure is caused by the damage due to the alpha particles emitted by radon progeny. Alpha particle is a positively charged particle which consists of two protons and two neutrons and emitted in radioactive decay or nuclear fission which is the nucleus of a helium atom. It is one of the radon decay products that responsible to deliver the actual radiation dose to lung tissue. When the radon progeny is trapped in the human lung, it will emit ionizing radiation in the form of alpha particles in which can damage the cell lining of the airways. The alpha particles are derived from the decay of Uranium-238 into Thoron-234

$$^{238}_{92}U \longrightarrow {}^{234}_{90}Th + {}^{4}_{2}He$$

Alpha particle

2.2 Building Materials Consisting of Rn-222

There are many building materials consisting of radon that can lead towards radiation. Most of the building materials contain amount of radionuclide in which will cause the internal and external radiation exposure. The doses of radiation from building materials vary depending on the natural radionuclides of ^{226}Rn, ^{232}Th, ^{40}K present in them. From the research by Kathren (1998),building materials is one of the Naturally Occurring Radioactive Materials (NORM).

Based on the rate of emanation, building materials can be divided randomly into two groups which are materials used for processing at high temperature as well as red brick, ash, cement and also slag. The other type is the materials that do not expose towards high temperature during processing such as silicate brick, gravel and sand, with 10 times higher in emanation rate. When the red brick is transformed into powder form in larger fragment, the rate of radon emanation can be determined easily. Thus, an estimation rate of emanation can be determined when it is in solid form. The component of building materials includes the red brick that is made from clay, stone and cement in which will contribute to Rn-222 emanations.

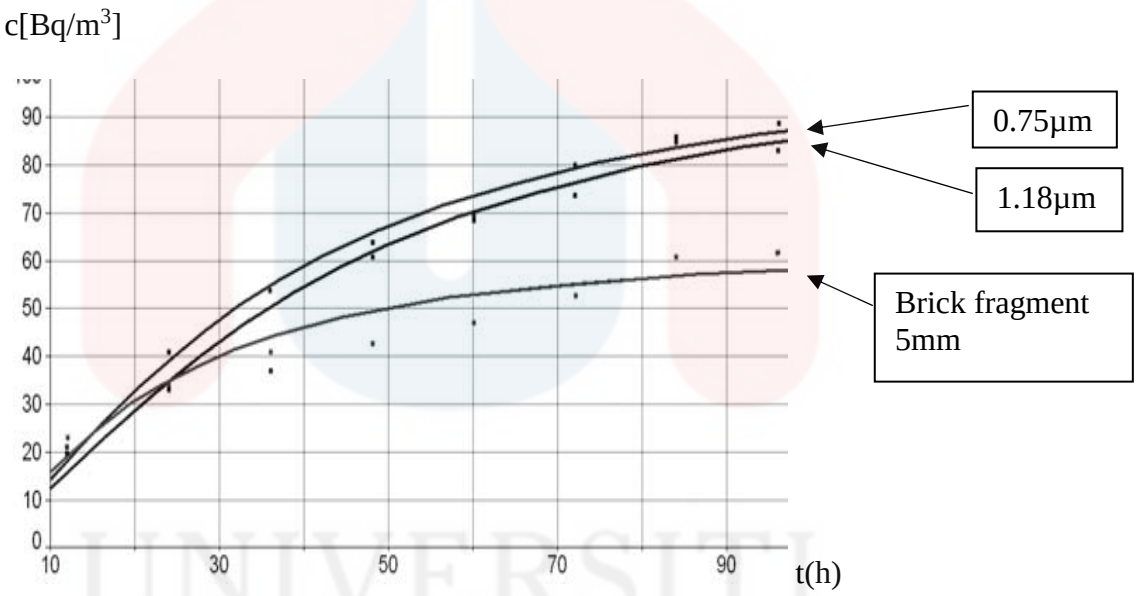

Figure 2.3: Example of Rn-222 emanation from red brick in fragment (Kaiser, 1999)

Table 2.1: By-product of radon concentration in red brick (Kaiser, 1999)

Materials	**Typical Activity Concentration (Bq kg^{-1})**			**Maximum Activity Concentration (Bq kg^{-1})**		
By-Product	^{226}Ra	^{232}Th	^{40}K	^{226}Ra	^{232}Th	^{40}K
Red Brick	50	50	670	200	200	2000

2.2.1 Stone

In order to form one bulk of the bricks, the stone is one of the materials used to form the bricks with the right composition. As Radon can be found in building materials, stone also consists of its own quantity of radon in which act as the attenuators of gamma rays emitted outdoors. Throughout the combination of stone to form the bricks, the amount of radon might be more as radon can also be found in the bricks. According to (Barton & Ziemer, 1986) the concentration of radon from stone dust is depending on the climatic factors, weather conditions and the type of dust.

2.2.2 Clay

Clay is one of the unique natural formations consisting of fine clay minerals and colloids materials which are metal hydroxide and organic matter. All of the compositions in the formation of the clay have made it radically different with other type of building materials that consist of radon. Clay consists of four different types of microstructure which are cellular, matrix, turbulent and laminar. Microstructure of clay plays an important role in determining the emanation capacity of radon. Each of the clay microstructure will emit different amount of radon concentration.

The combination of clay and borogypsum (BG) will be forming bricks which follow the American Society for Testing and Materials (ASTM) standards. The compressive strength of the brick indicates the improvement due to the addition of BG. The clays that are undergoing the burning process in making bricks will result in a better effective protection from gamma ray compared to other materials (Mann et al., 2016).

2.2.3 Cements

Cement is one of the main and important sources used in building constructions in many countries and it is used on a large scale. Cement is also used for making block, concrete and for plastering the building made from brick. By plastering the building made from bricks, it can reduce the emanation rate of Radon from the brick as the major source of Radon in building constructions. Meanwhile, cement is considered as one of the radiation source in indoor environment for Radon exhalation rates.

Porosity, pressure, grain size of the cement structure gives an effect during the production of cement will encourage large amount of Radon concentration emanates to the building environment.

2.3 Coating in Preventing Rn-222 Emanations

In this research, there is a way in controlling the emanation rate of the radon from being exposed to the surrounding. As the temperature, air pressure and humidity significantly influence the radon exhalation in dwelling, the covering materials that can be applied on the building material is red brick. The different types of coating or covering materials applied on building materials will result in a different emanation rate of radon concentration.

One of the types of coating system is paint which is consisting of different porosity. Thus, it can influence the different amount of radon emanation rate which is also exposed to environment. The finishing materials such as plaster, tile and paint indicate effectiveness in the reduction of indoor radon (Ma et al., 1995).

2.3.1 Coating Layers in Preventing Emanation of Radon

Paint can alos prevent the emanation of Radon from the building materials. Multilayer of coating formed with the combination of attractive properties of several materials can help solve the problem in any types of application. In this case, coating is used to minimize the emanation of Radon from the building materials to the surrounding.

Multilayer of coating is more preferable rather than single layer of coating due to its better scale adherence. There is a close relationship between adhesion properties of coating layers in TBC (Thermal Barriers Coating) where it is applied to protect the metallic components exposed to the high thermal gradients in applications. Besides acting as an anticorrosion agent, it can also improve the performance of the materials applied with the coating.

Thus, it can be concluded that the adherence of multilayer coating can lead to the decreasing amount of radon concentration from emanates to the surrounding of building materials. The failure of coating adhesion will also deteriorate the protective properties of coatings.

2.3.2 Effect of Porosity in Coating Materials

Coatings play an important role to minimize the emanation of Radon from the building materials to the surrounding. The degree of porosity of coating materials should be synchronized with the porosity of building materials since the building materials also has their own porosity.

Paint is one type of coating materials which is widely used in construction. Each type of paint has different composition and different porosity which will result in different amount of Radon emanation's concentration from the building materials

used (Ma *et al*., 1995). A higher porosity of coating materials will result in high rate of Radon concentration to the surrounding and more alpha particles will be emitted in which it is harmful towards human health.

Coating has the barrier properties and it is also capable of reducing the transmission of ultraviolet (UV) radiation due to its particles that have an excellent corrosion prevention and also UV resistance. Thus, Radon cannot be easily emanated to the surrounding since the coating has a good prevention mechanism.

2.3.3 Viscosity of Coating Materials

Radon emanation has a strong relationship with the viscosity of coating whereby higher coating viscosity will result in the low rate of Radon concentration from being emanated towards the surrounding. Particularly, it is desirable to characterize the emulsion system including the chemical composition, heterogeneity, particle size, viscosity and any types of chemical and physical properties as the functions of coatings.

The viscosity of coating might be affected due to the widely used of cellulose ether polymers as the thickening agents in formation of paint. Biological contamination in raw materials, processing and storage facilities might also be the cause of the loss in coating viscosity. The interaction between oxidizing and reducing agents from excess of polymerization remaining in emulsion is the major cause of viscosity reduction in waterborne paint. Holmes (1969); Oppermann (1986) stated that the main route leading to the loss of coating viscosity is the contamination of emulsion paint by microbial cellulolytic enzymes.

2.4 Adhesiveness of Coating Materials

Coating material plays an important role in preventing emanation of Rn-222. Thus, it can be high in strength and has long durability in order to be a good resistance from Radon emission towards the surrounding. Adhesion testing is the most suitable method in measuring the strength and durability of the coating materials used. ASTM, American Society for Testing and Materials defined adhesion as the region in which two surfaces are held together by interfacial forces which may consist of valence forces or interlocking forces or both.

The forces involved might be Van Der Waals or electrostatic forces and the interaction between coating and substrate might be good (P.R.Chalker, 1991). Thus, the high electrostatic forces will determine the strength of the coating materials and reduce the emanation of Rn-222.

The coating materials is said to be useless without sufficient adhesion although the coating have excellent properties of resistance to weather, scratch or impact (Tracton, 2005).

CHAPTER 3

MATERIALS AND METHODOLOGY

3.1 Study Area

This study was conducted in the lab of Materials Technology. In order to record the amount of radon in red brick, this research is conducted in the Material Science lab in UMK Kampus Jeli. All of the parameters involving the measurement of Rn-222 concentration in red brick were placed in the prototype room with the measurement of $40\times40\times40\times40cm^3$ cubic.

Figure 3.1: Area for measurement of Rn-222 concentration

Figure 3.1 shows the area for the measurement of Rn-222 concentration which is located at the back of the materials technology laboratory. The area was selected to maintain the humidity because there is no air-conditioner near the area and it is also far from the source of ultraviolet (UV) which is the sunlight. The source of sunlight can affect the reading of Rn-222 concentration.

3.2 Research Materials

The materials used in this research are known as red brick due to the common use in the construction sites as building materials. The materials used as in Figure 3.2 are the common building materials used in construction. The building materials were then applied with the layer of plaster to reduce the emanation rate of Rn-222. The plaster is made from the source of soil and it might contain the least amount of the Rn-222.

Figure 3.2: Ordinary red brick with standard size of 8x4 cm^3

Besides, the other material used in conducting this research is the cement in which act as the medium for plaster. The thickness of plaster is within the range of 0.5mm-2.0mm when applied on the red brick surfaces. The plastering process for each of the bricks required 1265.27g of cements. Figure 3.3 shows the cement used as plaster layer on the red bricks.

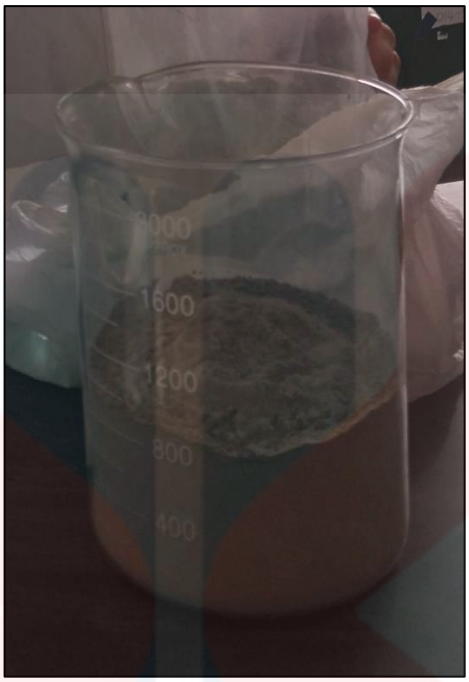

Figure 3.3: Type of cement used

Three different types of paint had been used in this project as the coating materials in preventing emanation of Rn-222. As shown in Table 3.1, the selected paint was used with the different assumption of viscosity to reduce the emanation rate of Rn-222. Each of coating materials was weighed for 64.53g in order to coat the surface of brick with plaster completely.

The coating materials used were consisting of different types and characteristics of composition and viscosity. The composition of each coating materials used was shown in Table 3.2 for the composition of Jotun, Table 3.3 for the composition of Nippon Paint and Table 3.4 for the composition of Dulux coating materials. The viscosity of each type of coating materials was measured by using the Stoke's Law method.

Table 3.1: Type of coating with assumption of viscosity

Paint Brand	Viscosity
Nippon Paint	High
Dulux	Low
Jotun	Medium

Table 3.2: Composition of Jotun Coating Type

No.	Elements
1	Diuron
2	Ammonia
3	Poly (oxy-1,2-Ethanediyl), Alpha-Nonylphenyl-Mega-Hydoxy-
4	5-Chloro-2-Methyl-4-Isothiazolin-3-One
5	2-Methyl-2H-Isothiazol-3-One

Table 3.3: Composition of Nippon Paint Coating Type

No.	Additives	Elements
1	Pigment	Mainly Titanium Dioxide(TiO_2), Iron Oxide(Fe_2O), Carbon(C), Black and Organic Pigments and Mineral Extender
2	Binder	All Acrylic
3	Thinner	Water

Table 3.4: Composition of Dulux Coating Type.

No.	Elements	(%)
1	Naphta (Petroleum), Hydreated Heavy	10-25
2	Talc, Magnesium Silicate	2.5-10
3	Distillates(Petroleum), Hydrated Light	2.5-10
4	Iodo Propynyl Butyl Carbonate	<1.5
5	Ethyl Methyl Ketoxime	<1.5

Figure 3.4: Amount of water used in preparing plaster

Water was used in conducting the project whereby it acted as the last medium in preparing the plaster. Figure 3.4 shows the amount of water used to prepare the plaster. The total volume of water that had been used in applying the plaster for the whole bricks was 750ml.

3.3 Research Equipment

The equipment involved in conducting this research was Radon Sentinel 1030 as shown in Figure 3.5. The concentration of Rn-222 was measured in passive and active ways. The passive ways were measured by collecting the sample concentration over a period of time. After that, it was taken away to be analysed while the active forms measured the Rn-222 concentration in a portion of spaces, resulting in the required outcome.

This device was originally purchased from sun nuclear in USA in summer 2014. It is approved by the Environmental Protection Agency (EPA) in which it will help to detect the emission of alpha particles from the decay of radon and its progeny.

A quick and accurate result as according to the specification is provided in the Appendix D.

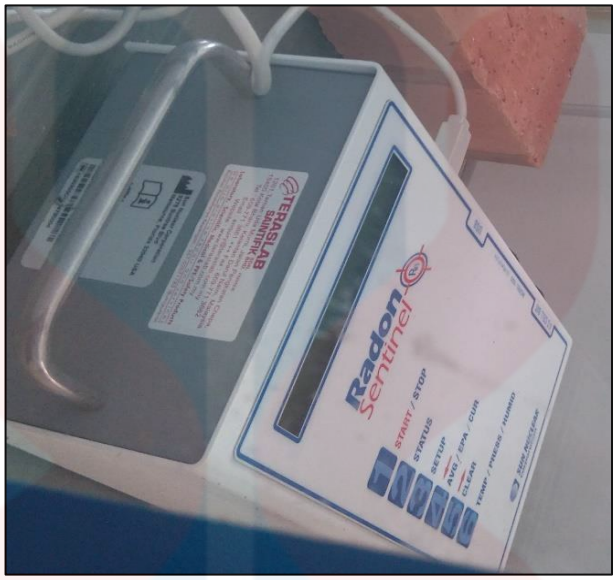

Figure 3.5: Radon Sentinel 1030

In order to measure the thickness of paster and the coating materials, the Vernier calipers as shown in Figure 3.6 were used. It is one of the tools with high-resolution length measurement. It also consists of two graduated scales.

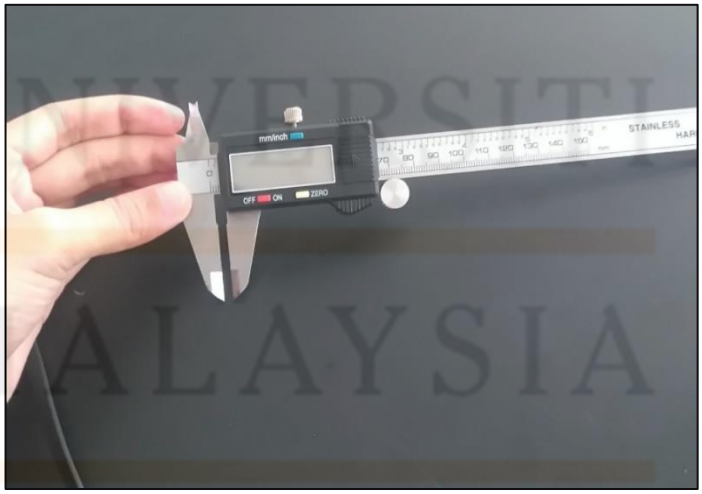

Figure 3.6: Standard Vernier callipers

In measuring the adhesiveness of the coating materials that have been used, adhesion tester was used to determine the strength and durability of the coatings. Figure 3.7 shows the adhesion tester used in this research. This equipment comes with 20 mm size of dolly complete with the grinder, glue and other requirement needed to handle this equipment.

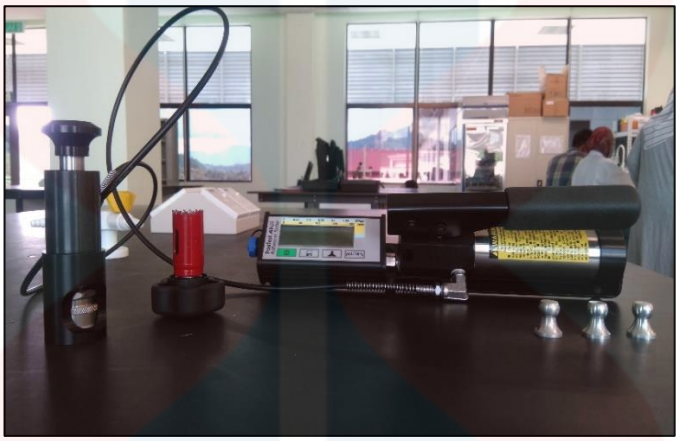

Figure 3.7: Adhesion tester

As shown in Figure 3.8, the prototype room was used as the medium to place the building materials and measure the concentration of Rn-222. This prototype was used to maintain the humidity, ventilation rate, temperature and humidity. Besides, this room will prevent air from entering the room.

Figure 3.8: $40cm^3 \times 40cm3 \times 40cm^3 \times 40cm^3$ perspex prototype room

3.4 Methods

3.4.1 Plaster Preparation

In preparing the plaster, cement, sand, and water were used to form the plaster which was then placed on the red brick surface. Figure 3.9 shows the steps involved in preparing the plaster to be coated on the brick surface according to the formula in Table 3.5.

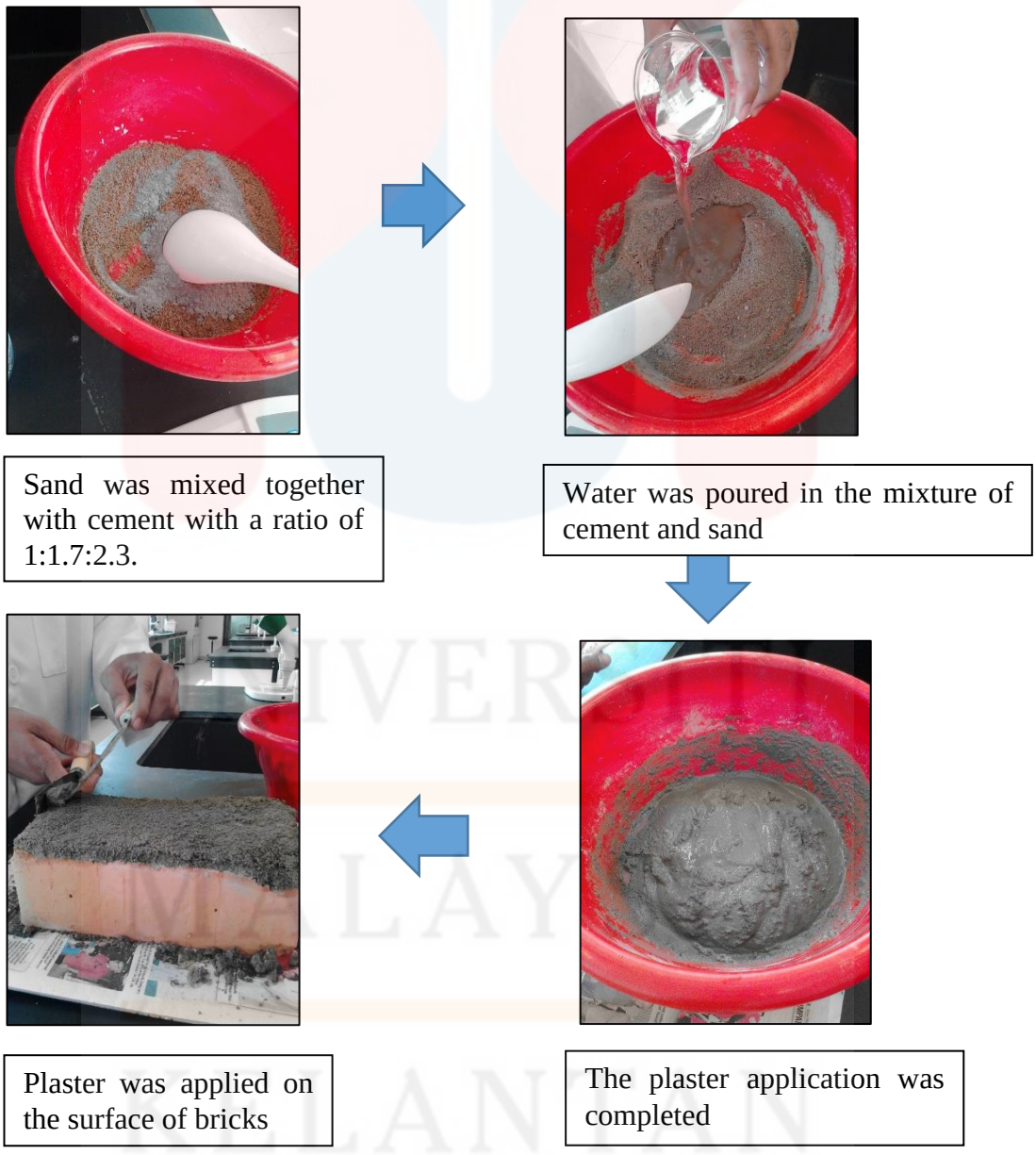

Figure 3.9: Process of plaster preparation

Table 3.5: Ratio for raw materials of plaster

Raw materials	Water	Cement	Sand
Ratio	1	1.7	2.3
Weight (g)	750	1265.27	1725.29

3.4.2 Coating Process

The coating process was conducted when the brick's entire surface is fully coated with the plaster. Different types of coating materials were used to prevent the emanation of Rn-222. Figure 3.10 shows the steps involved in applying the coating materials on the surface of bricks that had been fully applied with the plaster.

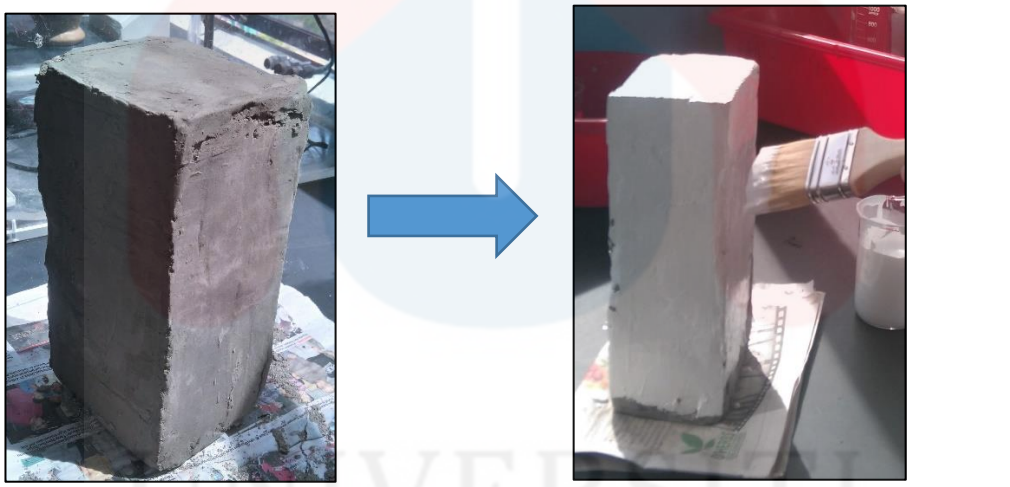

Figure 3.10: Applying coating process

3.4.3 Measuring the Concentration of Rn-222

The concentration of Rn-222 was measured after the brick was fully coated with the coating materials. The coated brick with selected coating materials was placed

in the prototype room with the presence of Radon Sentinel 1030 monitor. The raw materials involved had also been placed in the same room to measure the concentration of Rn-222. It was measured for only one day each. Figure 3.11 shows the method in measuring the concentration of Rn-222.

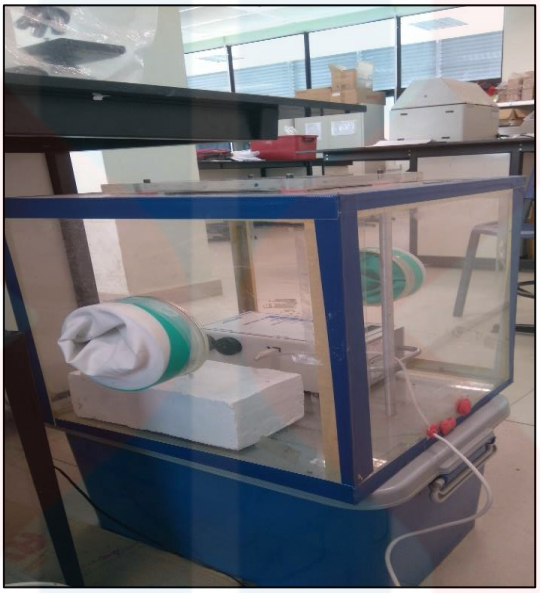

Figure 3.11: Measurement of Rn-222 concentration

3.4.4 Data collection

The measurement of Rn-222 concentration from this research was collected in two months' period due to the two types of data that should be collected which are the raw data and the main data. Both of the data was collected within 24 hours beginning at 8.00 a.m. to 10.00 a.m. with different interval and 0 hour of delay. For the raw data, there were nine types of raw materials involved. The raw materials involve were the empty room prototype, empty beaker, sand, cement, water, empty brick without plaster and coatings, and three types of selected coating which were Jotun, Dulux, and Nippon Paint.

The main data was including the brick with plaster, brick with plaster and Jotun coating type, brick with plaster and Dulux coating type and the brick with plaster and Nippon Paint coating type. The materials involved in measuring the concentration of Rn-222 were placed in the prototype room with Radon Sentinel monitor. The data gained in 24 hours was transferred from the monitor device to a personal computer via USB cable.

Table 3.6: Collection of raw data

Type of Raw Materials	Date
Prototype room	8/8/2016
Red brick	9/8/2016
Empty beaker	14/8/2016
Sand	15/8/2016
Cement	16/8/2016
Water	21/8/2016
Coating (Jotun)	22/8/2016
Coating (Nippon paint)	20/9/2016
Coating (Dulux)	27/9/2016

Based on Table 3.6, the collection of nine concentration of Rn-222 in raw materials started on 8/8/2016 to 27/9/2016. The collected data was classified as the raw data. It took 24 hours of duration and 0.5 intervals.

Table 3.7: Collection of main data

Main Data	Day (Date)				
	Day 1	Day 2	Day 3	Day 4	Day 5
Brick+Plaster	24/8/16	25/8/16	27/8/16	18/9/16	19/9/16
Brick+Plaster+Jotun	28/9/16	29/9/16	3/10/16	4/10/16	5/10/16
Brick+Plaster+Nippon	7/10/16	9/10/16	10/10/16	11/10/16	12/10/16
Brick+Plaster+Dulux	14/10/16	15/10/16	16/10/16	17/10/16	18/10/16

There were four main data of Rn-222 concentration collected starting from 24/8/2016 until 18/10/2016 as shown in Table 3.7. The collected data was classified as the main data. It took 24 hours of duration and 1-hour interval for each day.

3.4.5 Data Analysis

The radon monitor device was stopped after 24 hours of measurement for the raw data and also the main data. Thus, the obtained data were then transferred to a personal computer. The data gained has included the Rn-222 concentration in each 30 minute for raw data and in each 1 hour for main data throughout 24 hours of duration with the selected temperature (in Fahrenheit), humidity (%) and pressure (inHg). The temperature and pressure were then converted into degree Celsius (˚C) and Pascal (Pa) for table and graph fitting.

3.4.6 Adhesion tester determination

The coated surface of brick with selected coating materials' strength and durability was the main concerned in this study. First of all, the dolly was attached on the coated surface with glue and was left to dry. The circle shape was grinded around

the strongly attached dolly to enable the gauge attached to pull the dolly. When the dolly was fully attached to the gauge, the handler was pull-pushed to control the pressure which was shown on the screen.

The collected pressure was then transferred to a personal computer using the USB cable to get the average pressure used to pull off the coating materials on the brick surface. Figure 3.12 shows the way in determining the adhesiveness of coating materials.

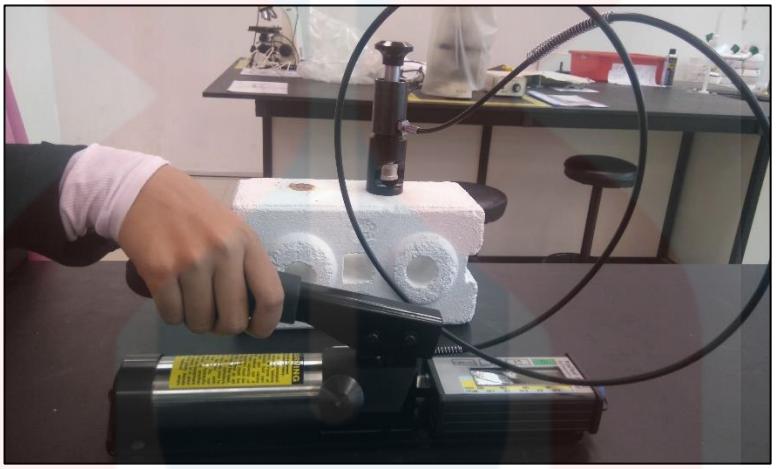

Figure 3.12: Determination of coating adhesiveness

3.4.7 Measurement of Coating Viscosity

The viscosity of each coating type was determined by using the formula adapted from the Stoke's Law:

$$\eta = \frac{2}{9}\left[(\rho 2 - \rho 1)(g)\left(\frac{r^2}{v}\right)\right] \qquad (3.1)$$

The measurements were consisting of the ball bearing, plastic measuring cylinder, 3 different types of coating materials, stopwatch, rope and metre ruler. The same volume of coating materials which is 100ml was poured in three different measuring cylinders. The ball bearing that had been tied with the rope was then

immersed in the coating materials. Subsequently, the time was taken and stopped until the ball bearing had reached the bottom of measuring cylinder. Figure 3.13 shows the process to measure the viscosity of each coating materials.

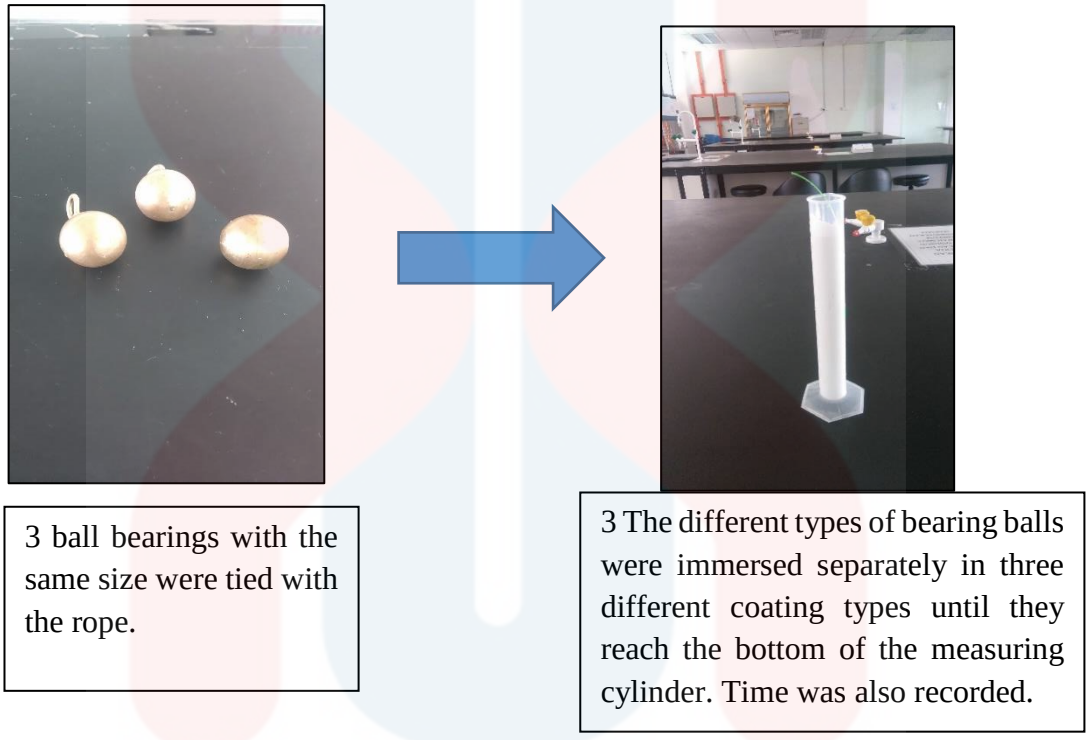

Figure 3.13: Measurements of Coating Viscosity

CHAPTER 4

RESULTS AND DISCUSSION

4.1 Emanation of Rn-222 From Raw Materials

The Rn-222 concentration of raw materials was obtained completely throughout the 24 hours' data collection for each raw material. The data were collected within 24 hours starting from 8.00 a.m. to 10.00 a.m. with 0.5hours of interval. Theoretically, the raw materials involved were consisting of the Rn-222 concentration which is also the source of Radon.

4.1.1 Rn-222 of Raw Materials in Prototype Room

Figure4.1 shows all of the raw materials used in this research. They were placed in the prototype room which influenced to obtain different concentrations of Rn-222.

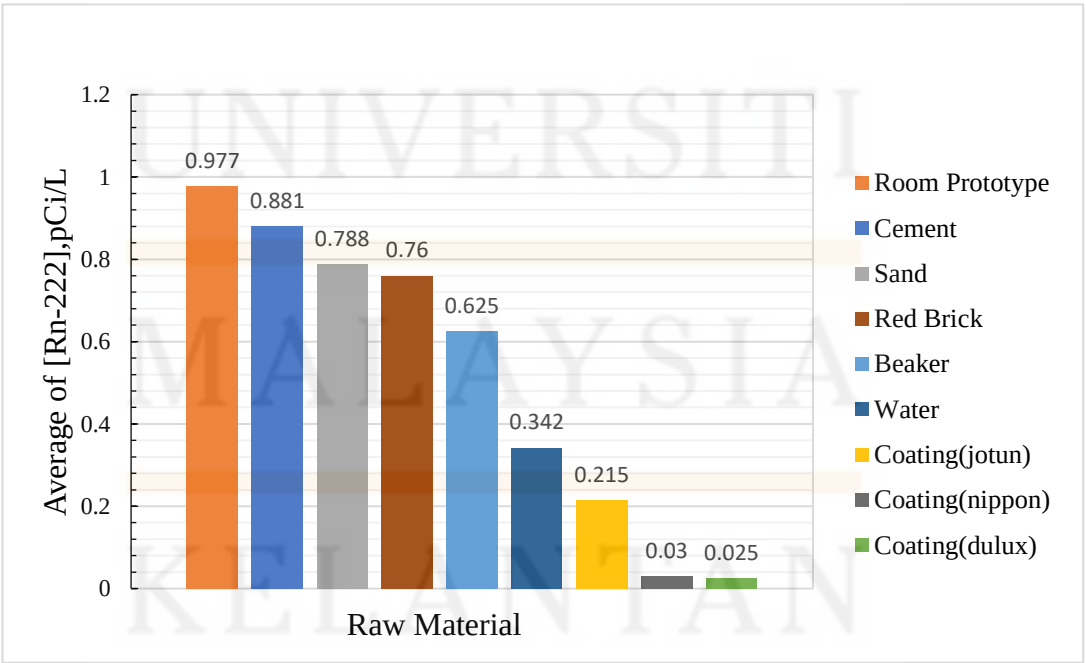

Figure 4.1: Average Rn-222 concentration of raw materials in prototype room

From Figure 4.1, prototype room recorded the highest rank of Rn-222 concentration. It can be concluded that low in humidity had the most effect on the concentration of Rn-222 in the prototype room. As the radiation is surrounding us, the radiation was also naturally occurring in the prototype room (H.Florou & P.Kritidis, 1992) mentioned that natural environmental radiation mainly depends on geological and geographical conditions. Although the Perspex box is considered as a vacuum container, there would be any fine and porous hole that influence the control space or air inside the box, hence affecting the consecutive Rn-222 reading of concentration.

Second highest rank of Rn-222 concentration was the cement specimen with 0.881 pCi/L concentration of Rn-222. Cement is considered as being widely used in developing countries and usually the gamma radiation level depends on the content of Ra, Th, and K in raw products (Bahi, 2004).

Sand is considered as having the highest concentration of Rn-222 which was 0.88 pCi/L. This is because sand exists naturally in soil and it contains high concentration of Rn-222. It is considered as the materials which cannot be exposed to high temperature due to its 10-20% emanation rate of Rn-222 concentration (Bikit et al., 2011). During the measurement of Rn-222 in sand, the humidity was around 75.02% resulting in low ventilation rates. Thus, Rn-222 emanates easily from the sand and enters the surrounding through common ways (Kullab, 2005).

The combination of sand, clay and stone will form bricks as building materials. The concentration of Rn-222 in red brick was 0.78 pCi/L and it can be classified as having a high concentration. The porosity structure in red bricks is allowing the Rn-222 to emanate freely from the bricks towards the surrounding. The weather during the measurement of Rn-222 concentration was quite hot, prompting a possibility of a higher concentration of Rn-222. Bikit et al. (2011) mentioned that bricks are

considered as the materials that are exposed towards high temperature during the production whereby it can contribute about 1-2% rate of Rn-222 emanation.

From Figure 4.1, Rn-222 readings for empty room prototype are conversely showing its concentration over the theoretical findings. The result should have indicated the lowest readings compared to other Rn-222 resources of Red Bricks, Empty beaker, Cement, Sand, and Water. This result might be due to the natural properties of Rn-222 gas which are random and having short half-life span (3.82 days). These properties directly influenced the data collected for consecutive days without the exchange of indoor air in the prototype room.

4.2 Emanation of Rn-222 in Red Brick

The concentration of Rn-222 in red brick was divided into 4 types of concentration which are the concentration of Rn-222 from brick with plaster, and the concentration from brick with plaster coated with different type of coating materials. The coating materials used were Jotun, Nippon Paint and Dulux.

Each of the different concentration parameters were measured in 5days with the duration of 24 hours and 1 hour of interval. In order to determine the effectiveness of plaster and coating type, minimum, maximum and nett concentration of each day were collected to plot the graph. Nett concentration was obtained by subtracting the collected concentration of each day with the concentration of the empty prototype room. Small amount of concentration determines the least amount of Rn-222 emanated from the Red Bricks.

4.2.1 Concentration of Rn-222 in Red Brick with Plaster.

The first concentration in Red Brick was measured with the presence of plaster on the surface of the Red Brick. The concentration was collected within 5 days starting from 24th August to 19th September 2016 in the duration of 24 hours each day. The obtained data was then calculated to get the nett Rn-222 concentration.

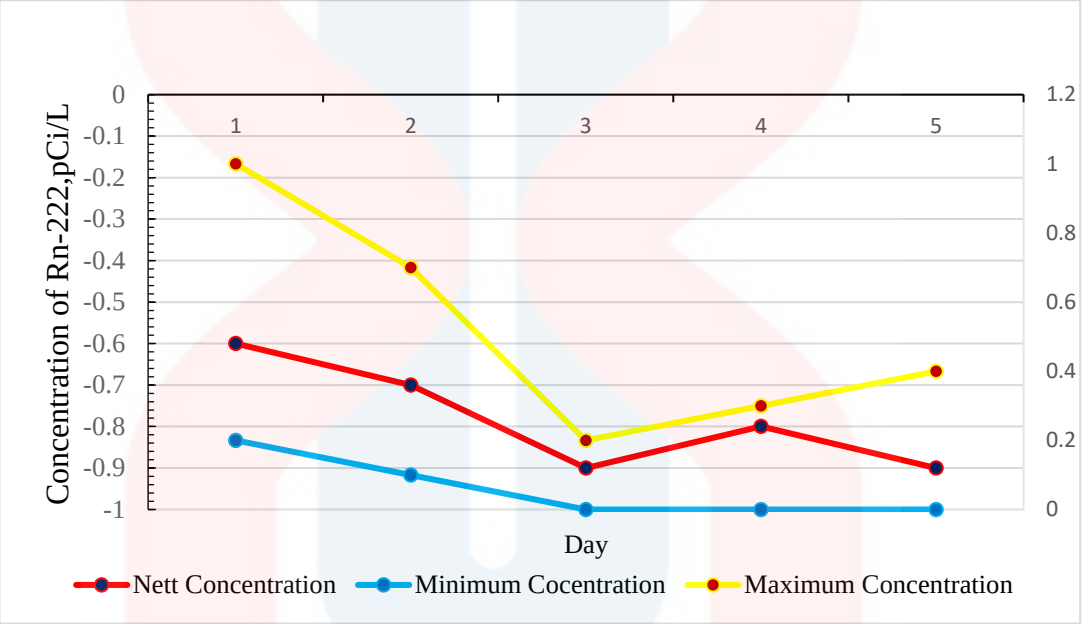

Figure 4.2: Nett, minimum and maximum concentration in Red Brick with Plaster

The collected result was then plotted as shown in Figure 4.2. Based on the graph, maximum concentration indicates the high range in between 0.8 pCi/L to 0.4 pCi/L while the minimum concentration is in between 0.2 pCi/L to 0 pCi/L. The concentration of each day was referred on the Appendix A.

The nett concentration was calculated by subtracting the collected concentration with the concentration in the empty prototype room. The nett concentration value was in between -0.6 pCi/L to -0.9 pCi/L. The concentration was increasing day by day due to the concentration activity of the natural radionuclides in by-product of building materials. There was a big variation between maximum and

minimum concentration and it might be caused by the different ventilation rate when the data was taken.

The plaster formed from the combination of sand and cement. Jang et al. (2014) said that cement is made from 40% of Granulated Blasted Furnace Slag (GBFS) with 2 - 4 times high concentration of Rn-222 than pure cementations materials. Thus, it is attributed towards high concentration of Rn-222 in red bricks after applying the plaster.

4.2.2 Concentration of Rn-222 in Red Brick with Plaster + Jotun Coating.

The next brick was applied with plaster followed the Jotun Coating. The concentration was collected within 5 day starting from 28th September to 5th October 2016 daily within 24 hours each day.

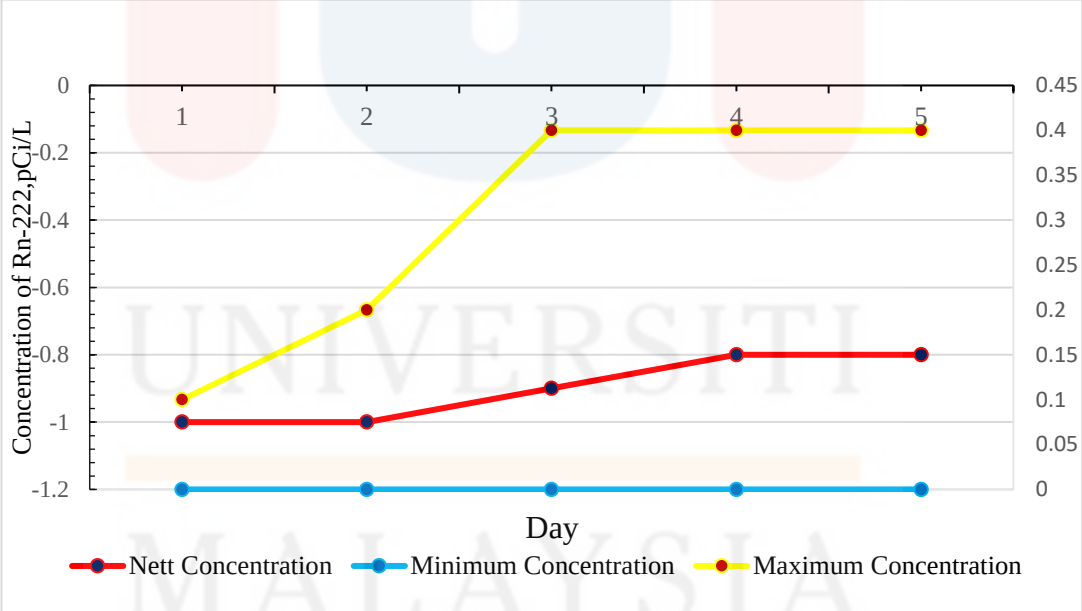

Figure 4.3: Nett, Minimum, and maximum concentration in Red Brick with Plaster coated with Jotun

The result was collected and plotted in graph (Figure 4.3). Based on the graph, maximum concentration was between 0.1 pCi/L to 0.4 pCi/L while the minimum

concentration remained constant within 5 days which is 0 pCi/L. Five consecutive concentration of Rn-222 was taken and shown in Appendix B.

The nett concentration collected was between -1.0 pCi/L to -0.9 pCi/L. The porosity of coating materials has allowed the Rn-222 to emanate from the bricks towards its surrounding. The applied coating materials reduced the emanation rate of Rn-222. The viscosity of Jotun coating materials was the second highest which was measured using Stoke's Law, reaching 149.58 Pa/s of viscosity.

The monitor did not detect the α-particle of radionuclide in building materials on the first and second day, possibly due to the random properties of Rn-222. The coating materials used should have the porosity in its structure even if it is considered as the effective medium in reducing the emanation of Rn-222.

4.2.3 Concentration of Rn-222 in Red Brick with Plaster + Nippon Paint Coating

The third concentration in red brick with plaster coated with Nippon Paint coating type was also measured within 5 days, with the duration of 24 hours daily. The concentration was measured starting from 7th October until 12th October 2016. The collected result was then plotted in graph (Figure 4.4).

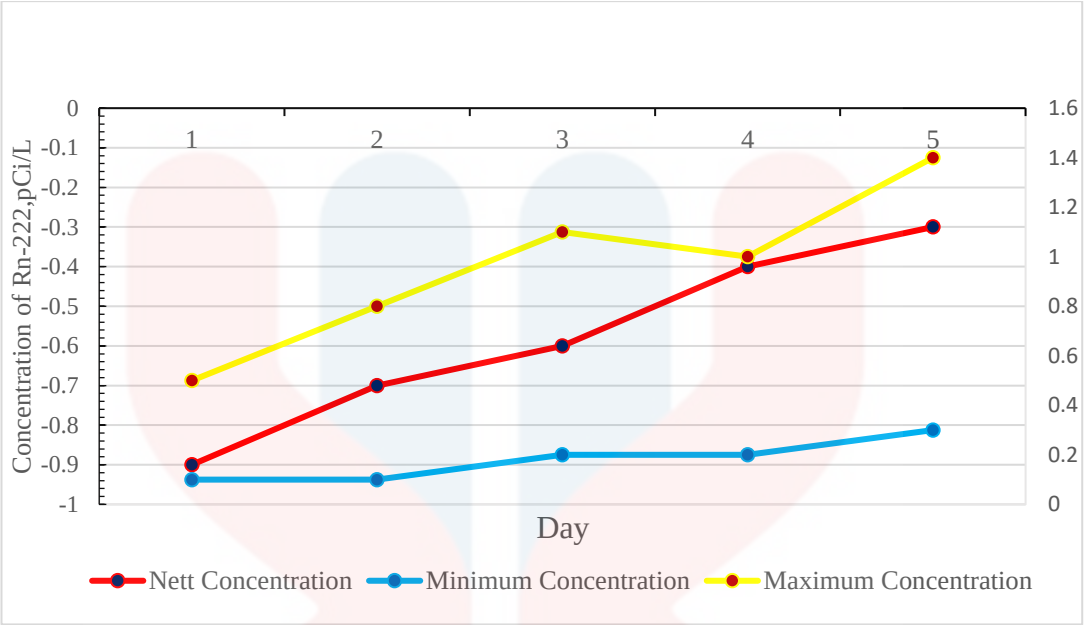

Figure 4.4: Nett, Minimum and Maximum concentration in Red Brick with Plaster coated with Nippon Paint

Based on the above Figure, maximum concentration has gradually increased in between 0.4 pCi/L to 1.1 pCi/L while the minimum concentration collected was between 0.1 pCi/L to 0.3 pCi/L. The collected nett concentration was between -0.9 pCi/L to -0.3 pCi/L within 5 days of data collection. The concentration taken for each day is shown in Appendix C.

The concentration was measured on 7th October during a rainy weather followed by a hot weather. Thus, the differences in weather condition were affecting the concentration of Rn-222. The monitor was detecting the least α-particles from the bricks day by day and the concentration of Rn-222 was also emanating slowly from the red bricks.

Besides, low emanation rate of Rn-222 from this red brick might be due to the coating materials of Nippon Paint application. According to the Stoke's Law, the viscosity of this type of coating materials was the highest compared with Jotun and Dulux coating type. This coating materials were mainly consisting of acrylic element

as the binder. Singh et al. (2005) mentioned that the compound of acrylic can be the effective medium in decreasing about 20 times the emanation of Rn-222 and acted as the barrier for Rn-222 to emanate in the environment.

4.2.4 Concentration of Rn-222 in Red Brick with Plaster + Dulux Coating.

The last concentration collected was the concentration of Red Brick with Plaster coated with Dulux coating type. The data was collected starting from 14thOctober until 18thOctober 2016. The collected result was then plotted in graph (Figure 4.5).

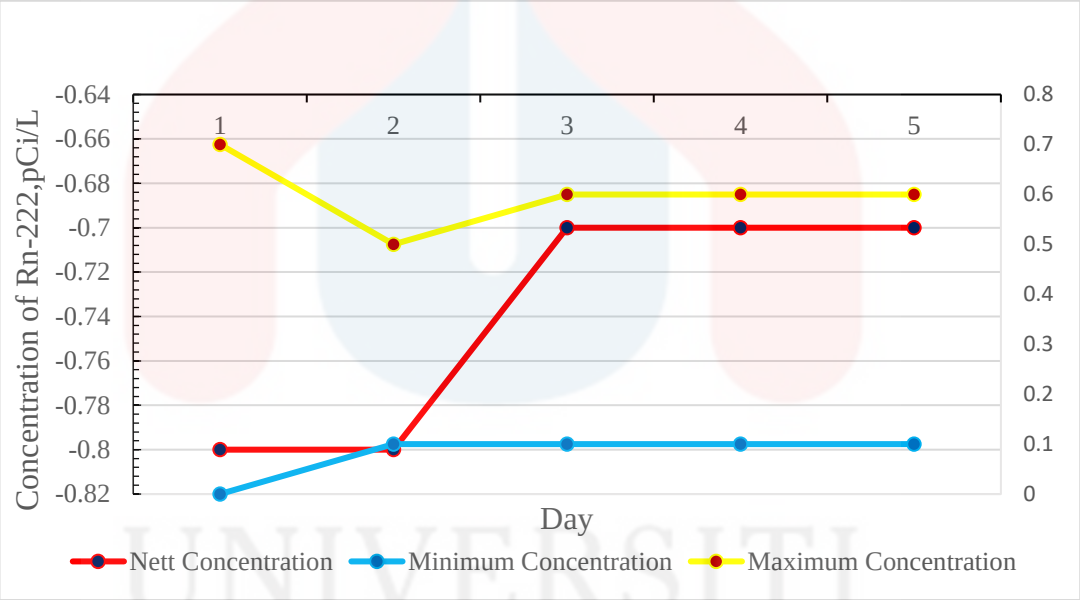

Figure 4.5: Nett, Minimum and Maximum concentration in Red Brick with Plaster coated with Dulux

Based on Figure 4.5, the maximum concentration had decreased on the second day from 0.7 pCi/L to 0.4 pCi/L. it was then constantly increasing to 0.5 pCi/L while the minimum concentration had also increased from 0 pCi/L on the first day and the next four days with 0.1 pCi/L. Meanwhile, the nett concentration collected was between -0.8 pCi/L to -0.7 pCi/L. Five consecutive concentrations for each day were taken and shown in Appendix D.

The monitor was randomly detected the α-particles of radionuclide as the random properties of radon and the existence of Rn-222 cannot be predicted to be existing every day. The exchange of environmental condition has caused the circuit in the Radon Monitor to be invincible from the presence of α-particles of the red bricks.

Thus, Dulux coating type was used to minimize the emanation of Rn-222 concentration from red bricks towards the surrounding. The different percentage of each composition in this coating type was one of the reasons of Rn-222 high emanation's concentration. According to the Stoke's Law, the viscosity of this coating type is the lowest rather than the other two type of coating materials.

4.3 Adhesive Testing

The durability and strength of coating was measured by undergoing the adhesive testing by using adhesive tester. Without sufficient adhesion, a coating or impact might be worthless. When the paint or coating materials is formulated, it must have a good adhesion features since the adhesion strength should be controlled after the coating has been spread on the substrate which is red brick with plaster (Tracton, 2005).

Table 4.1: Adhesion strength of coating materials

Type of coating	Pressure (psi)	Rate (psi/s)	Duration (s)
Jotun	190	56.03	1.97
Nippon paint	208	39.9	2.57
Dulux	130	115.1	0.28

The adhesion strength or effectiveness of coating materials used in reducing the emanation of Rn-222 from red brick was predicted based on Table 4.1. According to the table, the coating type of Nippon paint obtained the highest pressure in order to seal off the dolly from the coating materials attached on the substrate. Since the dolly

was hard to seal off from the surface of coating, the adhesion strength of coating is high. Thus, it is a good barrier to prevent emanation of Rn-222 from the red bricks.

4.4 Viscosity of Coating Materials

The emanation of Rn-222 can be reduced by applying the coating materials on the surface of the bricks. The coating materials with high viscosity are more effective in reducing the emanation of Rn-222 concentration towards the surrounding. Viscosity of coating materials was measured by using Stoke's Law.

The viscosity of coating materials was calculated by using the formula below:

$$\eta = \frac{2}{9}\left[(\rho 2 - \rho 1)(g)\left(\frac{r^2}{v}\right)\right] \quad (4.1)$$

Where,

η= Viscosity, ρ_2= Density of Coating Materials, ρ_1= Density of Ball Bearing, g= Standard Gravity, r = Radius of Ball Bearing and v= Ball bearing Velocity.

Table 4.2: Viscosity of coating materials using Stoke's Law.

Coating Materials	Mass (g)	Volume (ml)	Average Time (s)	Velocity (ms^{-2})	Viscosity(Pa/s)
Jotun	130.4	100	11.7	1.62	149.58
Nippon Paint	135.4	100	23.84	0.79	315.83
Dulux	106.84	100	3.2	5.94	33.37

Mass of Ball Bearing= 29.28g

Radius of Ball Bearing= 9.26

Based on table 4.2, each of the coating materials has their own viscosity and it was measured by using the Stoke's Law experiment. It can be observed that the

highest viscosity recorded from the Nippon Paint coating, followed by Jotun coating and Dulux coating.

The higher viscosity of coating can be considered as the most effective coating type in reducing the emanation of Rn-222. Nevertheless, the paint somehow will lose their viscosity as the thickening agents was used in degree of polymerization (Tothill & Seal, 1993).

CHAPTER 5

CONCLUSION AND RECOMMENDATION

5.1 Conclusion

According to the conducted research, the reduction of Rn-222 emanation from the Red Brick can be obtained by using the special characteristic of coating materials. The concentration of Red Brick before coated with the coating materials is between 0.2 pCi/L to 1.1 pCi/L. After it has been coated with coating materials, the concentration of Rn-222 seems to be decreasing with the range of -0.92 pCi/L coated with Jotun type, -0.55pCi/L coated with Nippon Paint type and -0.78pCi/L coated Dulux coating type. The concentration has decreased drastically after they were coated with different types of coating materials.

Coating materials used were consisting of different strength in reducing the emanation of Rn-222 in Red Bricks. After undergoing the adhesive testing and viscosity measurements, Nippon Paint coating is observed as the qualified coating material with high adhesion strength and having high viscosity due to the drastic decrease of Rn-222.

5.2 Recommendation and Future Study

Based on the result obtained from the study, the condition in the Materials Science laboratory should be improved whereby the air conditioner should be turned off while monitoring the Radon Sentinel 1030. Many instruments can affect the concentration reading such as XRD and X-Ray diffraction machine. The monitor can detect the alpha particles, as the XRD was also a major contributor towards radiation.

Future study can be done by recording each of the data in a longer period to get a more accurate result of Rn-222 concentration emission from the Red Bricks. Thus, more studies on the different types of bricks or other materials can be done in UMK Jeli Campus.

REFERENCES

Abdallah, S. M., Habib, R. R., Nuwayhid, R. Y., Chatila, M., & Katul, G. (2007). Radon measurements in well and spring water in Lebanon. *Radiation measurements, 42*(2), 298-303.

Aleissa, K. A., Alghamdi, A. S., Almasoud, F. I., & Islam, M. S. (2013). Measurement of radon levels in groundwater supplies of Riyadh with liquid scintillation counter and the associated radiation dose. *Radiat Prot Dosimetry, 154*(1), 95-103.

Bahi, S. M. E. (2004). Assesment of radioactivity and Radon Exhalation Rate in Egyptian Cement. *Health physics, 86*(5).

Barton, T., & Ziemer, P. (1986). The effects of particle size and moisture content on the emanation of Rn from coal ash. *Health physics, 50*(5), 581-588.

Bikit, I., Mrda, D., Grujic, S., & Kozmidis-Luburic, U. (2011). Granulation effects on the radon emanation rate. *Radiat Prot Dosimetry, 145*(2-3), 184-188.

Buonanno, G., Giovinco, G., Morawska, L., & Stabile, L. (2011). Tracheobronchial and alveolar dose of submicrometer particles for different population age groups in Italy. *Atmospheric Environment, 45*(34), 6216-6224.

Gosnell, T. B., & Wong, J. L. (2014). Rapid autonomous analysis of HPGe spectra II: Uranium identification and characterization.

H.Florou, & P.Kritidis. (1992). Gamma radiation measurements and dose rate in the coastal areas of a volcanic island,aegean sea,Greece. *Radiat Prot Dosimetry, 45*(1), 277-279.

Hay, A. (2015). Indoor Radon Exposure in British Columbia: A primer for health promotion.

Holmes, W. (1969). Housekeeping for latex paint manufacturing. *Journal of Paint Technology, 41*(539), 688-&.

Jang, H., Lee, M., Lee, M., & So, S. (2014). Monitoring Radon Concentration of Cement Mortar containing GBFS by Diffused Junction Photodiode Sensor. *International Journal of Software Engineering and Its Applications, 8*(2), 277-286.

Kaiser, S. (1999). Radiological Protection Principles Concerning the Natural Radioactivity of Building Materials. *Radiation Protection, 112*.

Kathren, R. L. (1998). NORM sources and their origins. *Applied radiation and isotopes, 49*(3), 149-168.

Kullab, M. (2005). Assessment of radon-222 concentrations in buildings, building materials, water and soil in Jordan. *Appl Radiat Isot, 62*(5), 765-773.

Ma, A., Man, C., Ho, E., & Pang, S. (1995). Effectiveness of finish materials and room air-conditioner on the reduction of indoor radon concentration in Hong Kong. *Radiation protection dosimetry, 60*(3), 237-241.

Mann, K. S., Heer, M. S., & Rani, A. (2016). Investigation of clay bricks for storage facilities of radioactive-wastage. *Applied Clay Science, 119*, 249-256.

Oppermann, R. (1986). *The anaerobic biodeterioration of paint.* Paper presented at the Biodeterioration 6: papers presented the 6th International Biodeterioration Symposium, Washington, DC, August 1984.

P.R.Chalker, S. J. B., &D.S Rickerby. (1991). A review of the methods for the evaluation of coating-substrate adhesion. *40*, 583-592.

Saad, A., Abdalla, Y., Hussein, N., & Elyaseery, I. (2010). Radon exhalation rate from building materials used on the Garyounis University campus, Benghazi, Libya. *Turkish Journal of Engineering and Environmental Sciences, 34*(1), 67-74.

Singh, S., Singh, J., & Singh, L. (2005). The study of some common plaster coating materials and plastic foils as a barrier to radon. *Radiation measurements, 40*(2-6), 673-677.

Somlai, K., Tokonami, S., Ishikawa, T., Vancsura, P., Gáspár, M., Jobbágy, V., Somlai, J., & Kovács, T. (2007). 222Rn concentrations of water in the Balaton Highland and in the southern part of Hungary, and the assessment of the resulting dose. *Radiation measurements, 42*(3), 491-495.

Tabar, E., & Yakut, H. (2013). Radon measurements in water samples from the thermal springs of Yalova basin, Turkey. *Journal of Radioanalytical and Nuclear Chemistry, 299*(1), 311-319.

Tothill, I., & Seal, K. (1993). Biodeterioration of waterborne paint cellulose thickeners. *International biodeterioration & biodegradation, 31*(4), 241-254.

Tracton, A. A. (2005). *Coatings Technology Handbook, Third Edition*: CRC Press.

Wang, Z., Lubin, J. H., Wang, L., Zhang, S., Boice, J. D., Cui, H., Zhang, S., Conrath, S., Xia, Y., & Shang, B. (2002). Residential radon and lung cancer risk in a high-exposure area of Gansu Province, China. *American Journal of Epidemiology, 155*(6), 554-564.

APPENDIX A

Table A.1: Data collected for first main data Rn-222 concentration in day 1

Time	[Rn-222]	Background,	Nett,	Temperature,	Temperature,	Pressure,	Pressure,	Pressure,	Humidity
	pCi/L	pCi/L	pCi/L	F	˚C	inHg	Pa	Pa×10^4	%
9:34AM	0.5	1	-0.5	83.5	28.61111111	29.8	100914.422	10.091	83
10:34AM	0.2	1.4	-1.2	82.4	28	29.8	100914.422	10.091	83
11:34AM	0.2	1.1	-0.9	81.9	27.72222222	29.8	100914.422	10.091	84
12:34PM	0.3	1.3	-1	81.9	27.72222222	29.7	100575.783	10.058	84
1:34PM	0.3	0.7	-0.4	81.7	27.61111111	29.7	100575.783	10.058	84
2:34 PM	0.2	1.1	-0.9	82.2	27.88888889	29.7	100575.783	10.058	84
3:34PM	0.5	1.2	-0.7	82.4	28	29.6	100237.144	10.024	84
4:34PM	0.4	0.7	-0.3	82.6	28.11111111	29.6	100237.144	10.024	84
5:34PM	0.5	1.6	-1.1	82.8	28.22222222	29.6	100237.144	10.024	83
6:34PM	0.7	1.4	-0.7	82.2	27.88888889	29.7	100575.783	10.058	84
7:34PM	0.4	1.3	-0.9	81.5	27.5	29.7	100575.783	10.058	84
8:34PM	0.4	1.2	-0.8	81.7	27.61111111	29.7	100575.783	10.058	84
9:34PM	0.3	1.4	-1.1	82.2	27.88888889	29.8	100914.422	10.091	84
10:34PM	0.6	0.7	-0.1	82.6	28.11111111	29.8	100914.422	10.091	84
11:34PM	0.6	0.5	0.1	82.8	28.22222222	29.8	100914.422	10.091	84
12:34AM	0.2	0.7	-0.5	82.9	28.27777778	29.8	100914.422	10.091	84
1:34AM	0.8	0.7	0.1	82.9	28.27777778	29.8	100914.422	10.091	84
2:34AM	0.3	0.8	-0.5	82.9	28.27777778	29.7	100575.783	10.058	84
3:34AM	0.3	1.1	-0.8	82.9	28.27777778	29.8	100914.422	10.091	84
4:34AM	0.5	1.2	-0.7	82.9	28.27777778	29.7	100575.783	10.058	84
5:34AM	0.7	0.4	0.3	82.8	28.22222222	29.8	100914.422	10.091	84
6:34AM	0.4	1	-0.6	82.8	28.22222222	29.8	100914.422	10.091	84
7:34AM	0.3	1.4	-1.1	82.6	28.11111111	29.8	100914.422	10.091	84
8:34AM	0.2	1	-0.8	82.6	28.11111111	29.8	100914.422	10.091	85

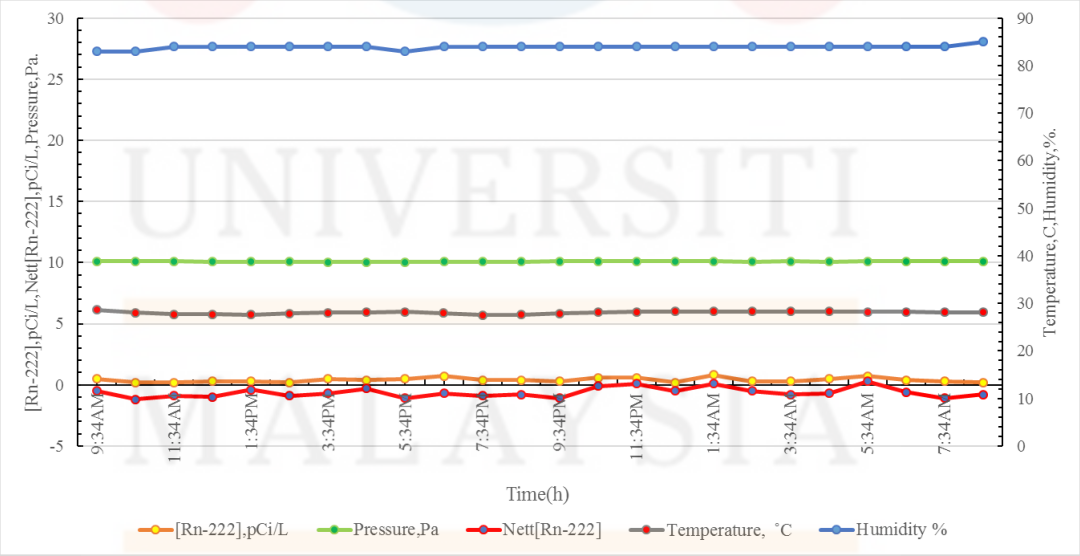

Figure A.1: Graph for first main data Rn-222 concentration in day 1

Table A.2: Data collected for first main data Rn-222 concentration in day 2

Time	[Rn-222],	Background,	Nett,	Temperature,	Temperature,	Pressure,	Pressure,	Pressure,	Humidity
	pCi/L	pCi/L	pCi/L	F	C	inHg	Pa	Pa×10^4	%
9:57 AM	0.3	1	-0.7	81.5	27.5	29.8	100914.422	10.091	84
10:57AM	0.4	1.4	-1	81.1	27.27777778	29.8	100914.422	10.091	85
11:57AM	0.5	1.1	-0.6	81.3	27.38888889	29.8	100914.422	10.091	85
12:57PM	0.3	1.3	-1	81.9	27.72222222	29.8	100914.422	10.091	84
1:57PM	0.2	0.7	-0.5	82.2	27.88888889	29.7	100575.783	10.058	85
2:57PM	0.4	1.1	-0.7	82.4	28	29.7	100575.783	10.058	84
3:57PM	0.5	1.2	-0.7	82.4	28	29.7	100575.783	10.058	84
4:57PM	0.2	0.7	-0.5	82	27.77777778	29.7	100575.783	10.058	84
5:57PM	0.4	1.6	-1.2	81.3	27.38888889	29.7	100575.783	10.058	85
6:57PM	0.2	1.4	-1.2	80.8	27.11111111	29.8	100914.422	10.091	85
7:57PM	0.1	1.3	-1.2	81.1	27.27777778	29.8	100914.422	10.091	85
8:57PM	0.2	1.2	-1	81.7	27.61111111	29.8	100914.422	10.091	85
9:57PM	0.2	1.4	-1.2	82	27.77777778	29.8	100914.422	10.091	85
10:57PM	0.4	0.7	-0.3	82.4	28	29.8	100914.422	10.091	85
11:57PM	0.4	0.5	-0.1	82.6	28.11111111	29.8	100914.422	10.091	85
12:57AM	0.6	0.7	-0.1	82.4	28	29.8	100914.422	10.091	85
1:57AM	0.3	0.7	-0.4	82.4	28	29.8	100914.422	10.091	85
2:57AM	0.5	0.8	-0.3	82.4	28	29.8	100914.422	10.091	85
3:57AM	0.2	1.1	-0.9	82.4	28	29.8	100914.422	10.091	85
4:57AM	0.4	1.2	-0.8	82.4	28	29.8	100914.422	10.091	85
5:57AM	0.3	0.4	-0.1	82.2	27.88888889	29.8	100914.422	10.091	85
6:57AM	0.5	1	-0.5	82.2	27.88888889	29.8	100914.422	10.091	86
7:57AM	0.4	1.4	-1	82	27.77777778	29.8	100914.422	10.091	85
8:57AM	0.6	1	-0.4	82	27.77777778	29.8	100914.422	10.091	85

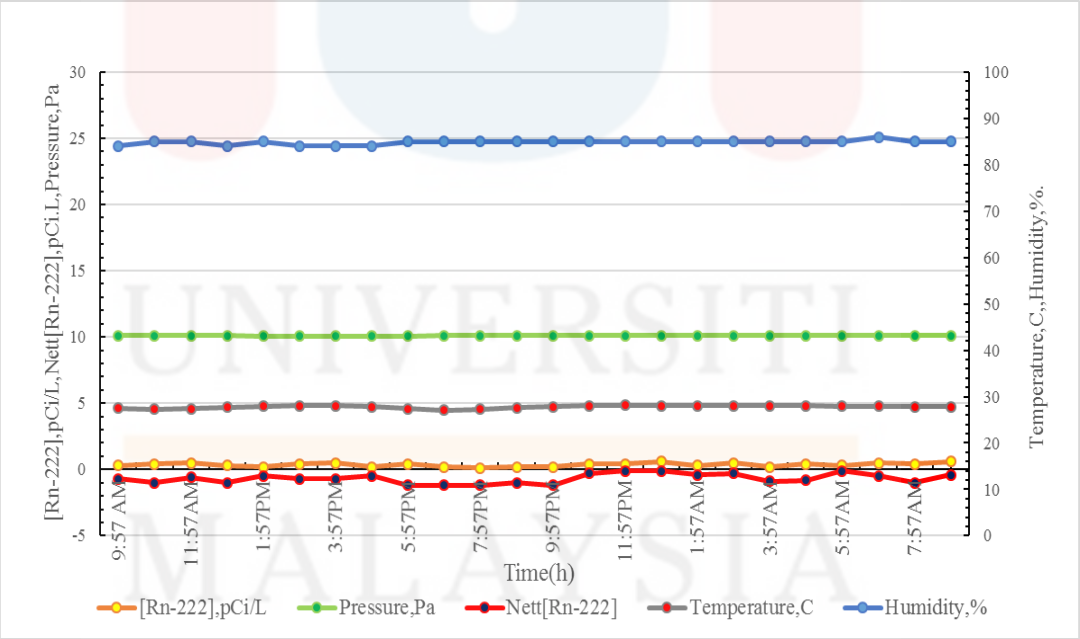

Figure A.2: Graph for first main data Rn-222 concentration in day 2

Table A.3: Data collected for first main data Rn-222 concentration in day 3

Time	[Rn-222],	Background,	Nett,	Temperature,	Temperature,	Pressure,	Pressure,	Pressure,	Humidity
	pCi/L	pCi/L	pCi/L	F	˚C	inHg	Pa	Pax10^4	%
9:03AM	0.1	1	-0.9	84	28.88888889	29.9	101253.061	10.125	85
10:03AM	0.1	1.4	-1.3	84.6	29.22222222	29.9	101253.061	10.125	85
11:03AM	0.2	1.1	-0.9	85.3	29.61111111	29.9	101253.061	10.125	85
12:03PM	0.2	1.3	-1.1	86	30	29.9	101253.061	10.125	85
1:03PM	0.2	0.7	-0.5	86.4	30.22222222	29.8	100914.422	10.091	85
2:03PM	0.1	1.1	-1	87.1	30.61111111	29.8	100914.422	10.091	85
3:03PM	0.2	1.2	-1	87.8	31	29.8	100914.422	10.091	85
4:03PM	0.1	0.7	-0.6	88.2	31.22222222	29.8	100914.422	10.091	85
5:03PM	0	1.6	-1.6	88.2	31.22222222	29.8	100914.422	10.091	85
6:03PM	0.2	1.4	-1.2	88	31.11111111	29.8	100914.422	10.091	85
7:03PM	0.2	1.3	-1.1	86.9	30.5	29.8	100914.422	10.091	86
8:03PM	0.1	1.2	-1.1	86.2	30.11111111	29.8	100914.422	10.091	85
9:03PM	0.1	1.4	-1.3	85.8	29.88888889	29.9	101253.061	10.125	86
10:03PM	0	0.7	-0.7	85.5	29.72222222	29.9	101253.061	10.125	86
11:03PM	0.1	0.5	-0.4	85.1	29.5	29.9	101253.061	10.125	86
12:03AM	0	0.7	-0.7	84.9	29.38888889	29.9	101253.061	10.125	86
1:03AM	0.1	0.7	-0.6	84.6	29.22222222	29.9	101253.061	10.125	87
2:03AM	0.1	0.8	-0.7	84.4	29.11111111	29.9	101253.061	10.125	86
3:03AM	0.1	1.1	-1	84.2	29	29.9	101253.061	10.125	87
4:03AM	0.1	1.2	-1.1	83.8	28.77777778	29.9	101253.061	10.125	86
5:03AM	0.1	0.4	-0.3	83.7	28.72222222	29.9	101253.061	10.125	87
6:03AM	0.1	1	-0.9	83.5	28.61111111	29.9	101253.061	10.125	87
7:03AM	0.1	1.4	-1.3	83.3	28.5	29.9	101253.061	10.125	86
8:03AM	0.1	1	-0.9	83.1	28.38888889	29.9	101253.061	10.125	86

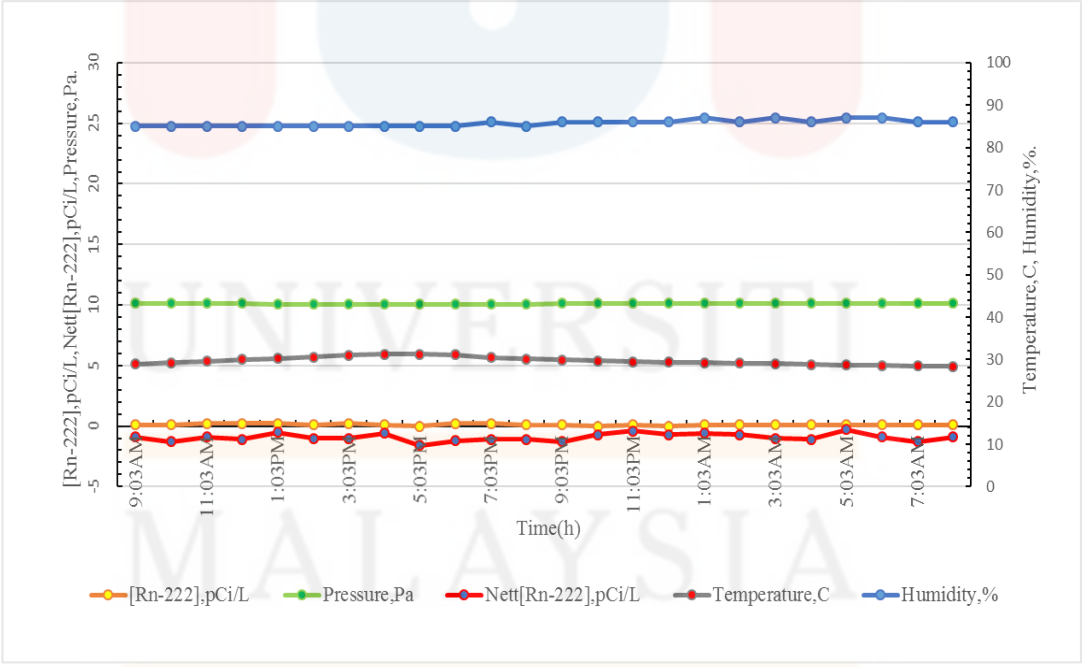

Figure A.3: Graph for first main data Rn-222 concentration in day 3

Table A.4: Data collected for first main data Rn-222 concentration in day 4

Date/Time	[Rn-222],	Background,	Nett,	Temperature,	Temperature,	Pressure,	Pressure,	Pressure,	Humidity
	pCi/L	pCi/L	pCi/L	F	°C	inHg	Pa	Pax10^4	%
9:11AM	0.2	1	-0.8	83.7	28.72222222	29.9	101253.061	10.125	75
10:11AM	0.1	1.4	-1.3	82.9	28.27777778	29.9	101253.061	10.125	77
11:11 AM	0.3	1.1	-0.8	82.4	28	29.9	101253.061	10.125	77
12:11PM	0.1	1.3	-1.2	82.2	27.88888889	29.8	100914.422	10.091	78
1:11PM	0.3	0.7	-0.4	82.6	28.11111111	29.8	100914.422	10.091	78
2:11PM	0.3	1.1	-0.8	82.6	28.11111111	29.8	100914.422	10.091	78
3:11PM	0.1	1.2	-1.1	82.6	28.11111111	29.8	100914.422	10.091	79
4:11PM	0.1	0.7	-0.6	82.6	28.11111111	29.8	100914.422	10.091	79
5:11PM	0.1	1.6	-1.5	82.6	28.11111111	29.7	100575.783	10.058	79
6:11PM	0.1	1.4	-1.3	82.2	27.88888889	29.8	100914.422	10.091	80
7:11PM	0.2	1.3	-1.1	81.7	27.61111111	29.8	100914.422	10.091	80
8:11PM	0	1.2	-1.2	80.8	27.11111111	29.8	100914.422	10.091	80
9:11PM	0.2	1.4	-1.2	79.9	26.61111111	29.8	100914.422	10.091	80
10:11PM	0.2	0.7	-0.5	79.2	26.22222222	29.8	100914.422	10.091	81
11:11PM	0.2	0.5	-0.3	78.4	25.77777778	29.8	100914.422	10.091	81
12:11AM	0.2	0.7	-0.5	78.8	26	29.8	100914.422	10.091	81
1:11AM	0.2	0.7	-0.5	79.7	26.5	29.8	100914.422	10.091	81
2:11AM	0.2	0.8	-0.6	80.4	26.88888889	29.8	100914.422	10.091	81
3:11AM	0.1	1.1	-1	80.8	27.11111111	29.8	100914.422	10.091	81
4:11AM	0.1	1.2	-1.1	81.1	27.27777778	29.8	100914.422	10.091	81
5:11AM	0.1	0.4	-0.3	81.3	27.38888889	29.8	100914.422	10.091	81
6:11AM	0.2	1	-0.8	81.3	27.38888889	29.8	100914.422	10.091	81
7:11AM	0	1.4	-1.4	81.5	27.5	29.8	100914.422	10.091	81
8:11AM	0.1	1	-0.9	81.5	27.5	29.8	100914.422	10.091	81

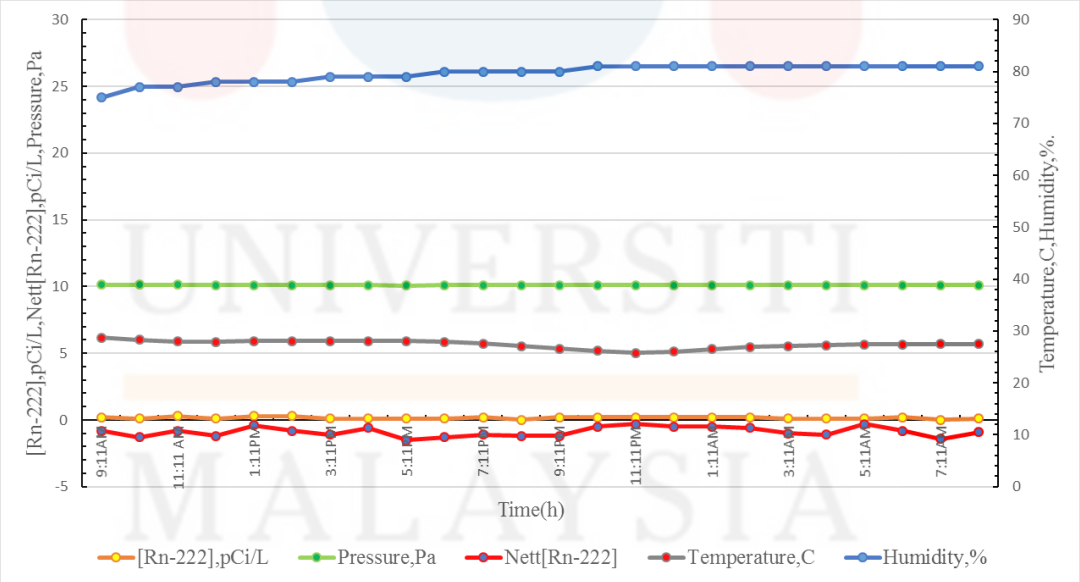

Figure A.4: Graph for first main data Rn-222 concentration in day

Table A.5: Data collected for first main data Rn-222 concentration in day 5

Date/Time	[Rn-222]	Background,	Nett,	Temperature,	Temperature,	Pressure,	Pressure,	Pressure,	Humidity,
	pCi/l	pCi/L	pCi/L	F	˚C	inHg	Pa	Pax10^4	%
9:24AM	0.1	1	-0.9	81.5	27.5	29.9	101253.061	10.125	81
10:24AM	0.4	1.4	-1	81.1	27.27777778	29.8	100914.422	10.091	81
11:24AM	0.1	1.1	-1	81	27.22222222	29.8	100914.422	10.091	82
12:24PM	0.1	1.3	-1.2	81.7	27.61111111	29.8	100914.422	10.091	82
1:24PM	0	0.7	-0.7	83.1	28.38888889	29.8	100914.422	10.091	80
2:24PM	0.2	1.1	-0.9	84.4	29.11111111	29.7	100575.783	10.058	81
3:24PM	0.1	1.2	-1.1	85.1	29.5	29.7	100575.783	10.058	81
4:24PM	0.1	0.7	-0.6	84.6	29.22222222	29.7	100575.783	10.058	81
5:24PM	0.2	1.6	-1.4	83.8	28.77777778	29.7	100575.783	10.058	81
6:24PM	0.2	1.4	-1.2	83.3	28.5	29.8	100914.422	10.091	82
7:24PM	0.4	1.3	-0.9	80.8	27.11111111	29.8	100914.422	10.091	85
8:24PM	0.1	1.2	-1.1	82.4	28	29.8	100914.422	10.091	82
9:24PM	0.1	1.4	-1.3	82.9	28.27777778	29.8	100914.422	10.091	82
10:24PM	0.1	0.7	-0.6	83.3	28.5	29.8	100914.422	10.091	82
11:24PM	0.2	0.5	-0.3	83.5	28.61111111	29.9	101253.061	10.125	82
12:24AM	0.1	0.7	-0.6	83.5	28.61111111	29.9	101253.061	10.125	82
1:24AM	0	0.7	-0.7	83.5	28.61111111	29.8	100914.422	10.091	82
2:24AM	0.1	0.8	-0.7	83.3	28.5	29.8	100914.422	10.091	82
3:24AM	0.1	1.1	-1	83.3	28.5	29.8	100914.422	10.091	82
4:24AM	0	1.2	-1.2	83.3	28.5	29.8	100914.422	10.091	83
5:24AM	0.1	0.4	-0.3	83.1	28.38888889	29.8	100914.422	10.091	83
6:24AM	0	1	-1	82.9	28.27777778	29.8	100914.422	10.091	82
7:24AM	0	1.4	-1.4	82.8	28.22222222	29.8	100914.422	10.091	83
8:24AM	0.1	1	-0.9	82.9	28.27777778	29.8	100914.422	10.091	83

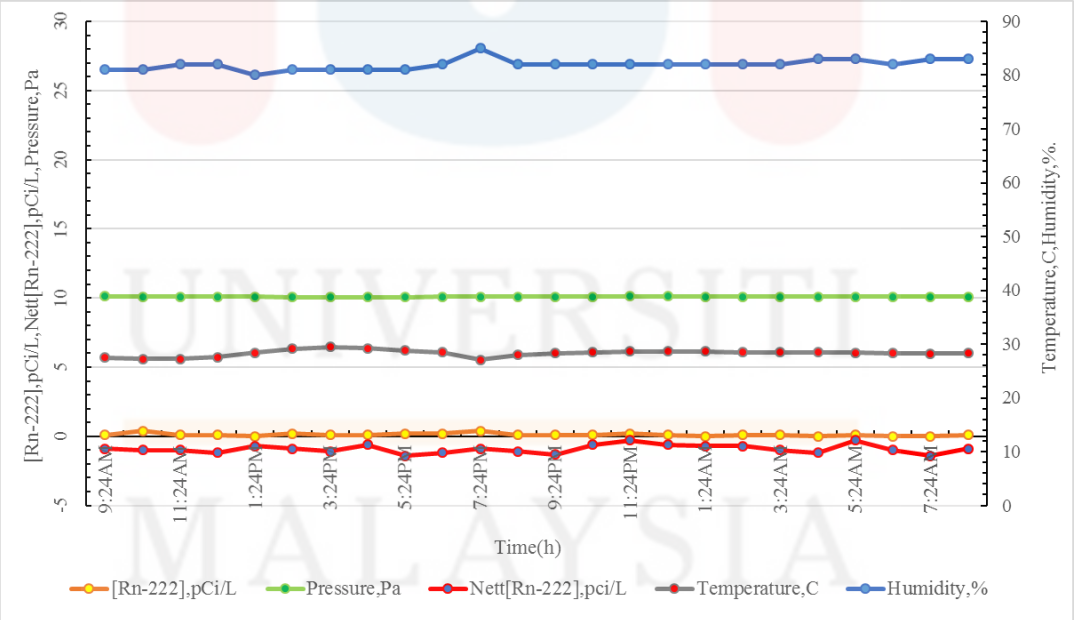

Figure A.5: Graph for first main data Rn-222 concentration in day 5

APPENDIX B

Table B.1: Data collected for second main data Rn-222 concentration in day 1

Date/Time	[Rn-222]	Background,	Nett,	Temperature,	Temperature,	Pressure,	Pressure,	Pressure,	Humidity
	pCi/l	pCi/L	pci/L	F	˚C	inHg	Pa	Pax10^4	%
9:43AM	0	1	-1	80.4	26.88888889	29.9	101253.061	10.125	82
10:43AM	0.1	1.4	-1.3	80.1	26.72222222	29.9	101253.061	10.125	82
11:43AM	0	1.1	-1.1	80.1	26.72222222	29.8	100914.422	10.091	82
12:43PM	0	1.3	-1.3	80.4	26.88888889	29.8	100914.422	10.091	82
1:43PM	0.1	0.7	-0.6	81	27.22222222	29.8	100914.422	10.091	82
2:43PM	0.1	1.1	-1	81.5	27.5	29.8	100914.422	10.091	82
3:43PM	0	1.2	-1.2	81.9	27.72222222	29.7	100575.783	10.058	83
4:43PM	0.1	0.7	-0.6	82	27.77777778	29.7	100575.783	10.058	82
5:43PM	0	1.6	-1.6	81.7	27.61111111	29.7	100575.783	10.058	82
6:43PM	0	1.4	-1.4	81.1	27.27777778	29.7	100575.783	10.058	82
7:43PM	0	1.3	-1.3	80.4	26.88888889	29.8	100914.422	10.091	83
8:43PM	0	1.2	-1.2	79.5	26.38888889	29.8	100914.422	10.091	83
9:43PM	0	1.4	-1.4	78.8	26	29.8	100914.422	10.091	82
10:43PM	0	0.7	-0.7	78.1	25.61111111	29.8	100914.422	10.091	83
11:43PM	0.1	0.5	-0.4	77.9	25.5	29.8	100914.422	10.091	83
12:43AM	0	0.7	-0.7	78.6	25.88888889	29.8	100914.422	10.091	82
1:43AM	0	0.7	-0.7	79.3	26.27777778	29.8	100914.422	10.091	83
2:43AM	0.1	0.8	-0.7	79.9	26.61111111	29.8	100914.422	10.091	83
3:43AM	0	1.1	-1.1	80.2	26.77777778	29.8	100914.422	10.091	83
4:43AM	0	1.2	-1.2	80.4	26.88888889	29.8	100914.422	10.091	83
5:43AM	0	0.4	-0.4	80.6	27	29.8	100914.422	10.091	82
6:43AM	0	1	-1	80.8	27.11111111	29.8	100914.422	10.091	82
7:43AM	0	1.4	-1.4	80.8	27.11111111	29.8	100914.422	10.091	83
8:43AM	0.1	1	-0.9	81	27.22222222	29.9	101253.061	10.125	82

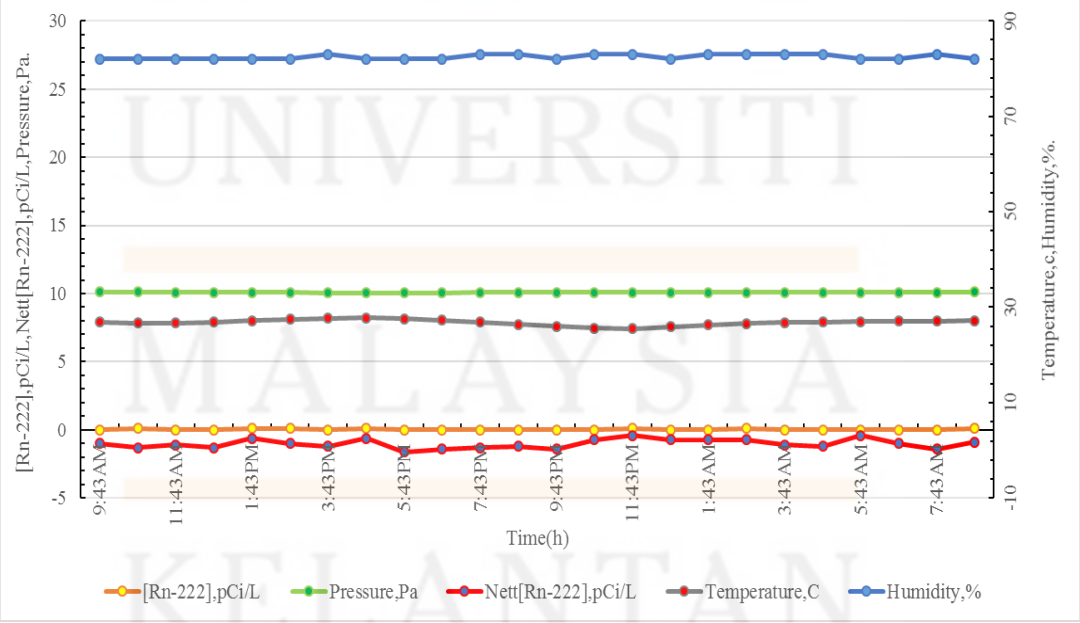

Figure B.1: Graph for second main data Rn-222 concentration in day 1

Table B.2: Data collected for second main data Rn-222 concentration in day 2

Date/Time	[Rn-222], pCi/l	Background, pCi/L	Nett, pCi/L	Temperature, F	Temperature, ˚C	Pressure, inHg	Pressure, Pa	Pressure, Pax10^4	Humidity %
9:46AM	0	1	-1	80.6	27	29.9	101253.061	10.125	82
10:46AM	0	1.4	-1.4	80.4	26.88888889	29.8	100914.422	10.091	82
11:46AM	0	1.1	-1.1	80.4	26.88888889	29.8	100914.422	10.091	82
12:46PM	0	1.3	-1.3	80.6	27	29.8	100914.422	10.091	82
1:46PM	0	0.7	-0.7	80.8	27.11111111	29.8	100914.422	10.091	82
2:46PM	0	1.1	-1.1	80.8	27.11111111	29.8	100914.422	10.091	83
3:46PM	0.1	1.2	-1.1	80.8	27.11111111	29.8	100914.422	10.091	83
4:46PM	0	0.7	-0.7	80.6	27	29.7	100575.783	10.058	81
5:46PM	0	1.6	-1.6	80.1	26.72222222	29.7	100575.783	10.058	82
6:46PM	0.1	1.4	-1.3	79.5	26.38888889	29.8	100914.422	10.091	83
7:46PM	0.1	1.3	-1.2	79	26.11111111	29.8	100914.422	10.091	83
8:46PM	0	1.2	-1.2	78.3	25.72222222	29.8	100914.422	10.091	83
9:46PM	0	1.4	-1.4	77.5	25.27777778	29.8	100914.422	10.091	83
10:46PM	0.1	0.7	-0.6	77	25	29.8	100914.422	10.091	83
11:46PM	0	0.5	-0.5	76.8	24.88888889	29.8	100914.422	10.091	82
12:46AM	0.1	0.7	-0.6	77.2	25.11111111	29.8	100914.422	10.091	83
1:46AM	0.2	0.7	-0.5	77.7	25.38888889	29.8	100914.422	10.091	83
2:46AM	0.1	0.8	-0.7	78.4	25.77777778	29.8	100914.422	10.091	83
3:46AM	0	1.1	-1.1	78.8	26	29.8	100914.422	10.091	82
4:46AM	0.1	1.2	-1.1	79	26.11111111	29.8	100914.422	10.091	82
5:46AM	0.1	0.4	-0.3	79.2	26.22222222	29.8	100914.422	10.091	82
6:46AM	0.1	1	-0.9	79.3	26.27777778	29.8	100914.422	10.091	82
7:46AM	0.1	1.4	-1.3	79.3	26.27777778	29.8	100914.422	10.091	83
8:46AM	0.1	1	-0.9	79.5	26.38888889	29.9	101253.061	10.125	82

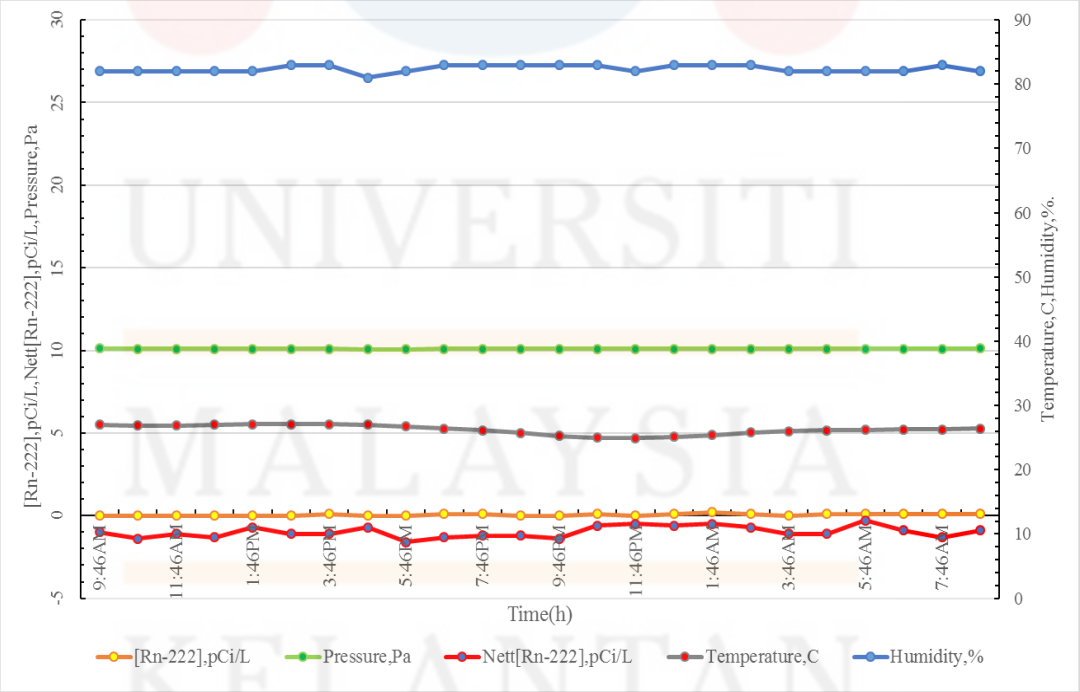

Figure B.2: Graph for second main data Rn-222 concentration in day 2

Table B.3: Data collected for second main data Rn-222 concentration in day 3

Date/Time	[Rn-222]	Background,	Nett,	Temperature,	Temperature,	Pressure,	Pressure,	Pressure,	Humidity
	pCi/l	pCi/L	pCi/L	F	˚C	inHg	Pa	Pax10^4	%
9:25AM	0	1	-1	85.5	29.72222222	29.9	101253.061	10.125	83
10:25AM	0	1.4	-1.4	85.1	29.5	29.9	101253.061	10.125	81
11:25AM	0.4	1.1	-0.7	84.9	29.38888889	29.9	101253.061	10.125	82
12:25PM	0.1	1.3	-1.2	85.1	29.5	29.8	100914.422	10.091	81
1:25PM	0.1	0.7	-0.6	85.3	29.61111111	29.8	100914.422	10.091	82
2:25PM	0	1.1	-1.1	85.3	29.61111111	29.8	100914.422	10.091	82
3:25PM	0.2	1.2	-1	85.3	29.61111111	29.8	100914.422	10.091	82
4:25PM	0	0.7	-0.7	85.3	29.61111111	29.8	100914.422	10.091	81
5:25PM	0.1	1.6	-1.5	84.7	29.27777778	29.8	100914.422	10.091	81
6:25PM	0.1	1.4	-1.3	83.8	28.77777778	29.8	100914.422	10.091	82
7:25PM	0	1.3	-1.3	82.9	28.27777778	29.8	100914.422	10.091	81
8:25PM	0	1.2	-1.2	82	27.77777778	29.8	100914.422	10.091	82
9:25PM	0.2	1.4	-1.2	81.1	27.27777778	29.8	100914.422	10.091	82
10:25PM	0.1	0.7	-0.6	80.4	26.88888889	29.9	101253.061	10.125	83
11:25PM	0.1	0.5	-0.4	80.6	27	29.8	100914.422	10.091	82
12:25AM	0.6	0.7	-0.1	81	27.22222222	29.8	100914.422	10.091	82
1:25AM	0.2	0.7	-0.5	81.5	27.5	29.8	100914.422	10.091	82
2:25AM	0.2	0.8	-0.6	81.7	27.61111111	29.8	100914.422	10.091	82
3:25AM	0.1	1.1	-1	81.9	27.72222222	29.8	100914.422	10.091	82
4:25AM	0	1.2	-1.2	81.9	27.72222222	29.8	100914.422	10.091	82
5:25AM	0.1	0.4	-0.3	81.9	27.72222222	29.8	100914.422	10.091	82
6:25AM	0.1	1	-0.9	81.9	27.72222222	29.8	100914.422	10.091	82
7:25AM	0	1.4	-1.4	81.7	27.61111111	29.8	100914.422	10.091	82
8:25AM	0	1	-1	81.7	27.61111111	29.8	100914.422	10.091	82

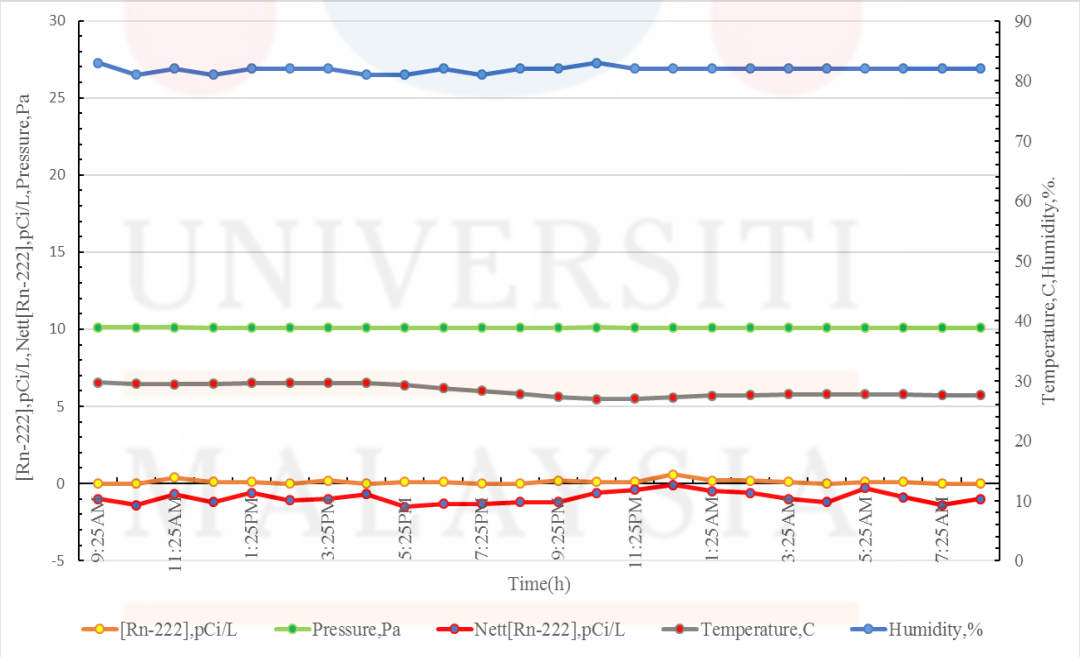

Figure B.3: Graph for second main data Rn-222 concentration in day 3

Table B.4: Data collected for second main data Rn-222 concentration in day 4

Date/Time	[Rn-222],	Background,	Nett,	Temperature,	Temperature,	Pressure,	Pressure,	Pressure,	Humidity
	pCi/l	pCi/L	pCi/L	F	˚C	inHg	Pa	Pax10^4	%
9:31AM	0.1	1	-0.9	81.5	27.5	29.8	100914.422	10.091	82
10:31AM	0.1	1.4	-1.3	81.3	27.38888889	29.8	100914.422	10.091	83
11:31AM	0.3	1.1	-0.8	81.5	27.5	29.8	100914.422	10.091	83
12:31PM	0.3	1.3	-1	81.5	27.5	29.8	100914.422	10.091	83
1:31PM	0.1	0.7	-0.6	81.7	27.61111111	29.8	100914.422	10.091	82
2:31PM	0	1.1	-1.1	81.7	27.61111111	29.8	100914.422	10.091	83
3:31PM	0.2	1.2	-1	82	27.77777778	29.7	100575.783	10.058	82
4:31PM	0.1	0.7	-0.6	82.2	27.88888889	29.7	100575.783	10.058	82
5:31PM	0.2	1.6	-1.4	82.4	28	29.7	100575.783	10.058	82
6:31PM	0.2	1.4	-1.2	82.2	27.88888889	29.7	100575.783	10.058	82
7:31PM	0.3	1.3	-1	81.5	27.5	29.8	100914.422	10.091	81
8:31PM	0.2	1.2	-1	80.6	27	29.8	100914.422	10.091	82
9:31PM	0.1	1.4	-1.3	79.7	26.5	29.8	100914.422	10.091	83
10:31PM	0.1	0.7	-0.6	79.2	26.22222222	29.9	101253.061	10.125	82
11:31PM	0.2	0.5	-0.3	78.4	25.77777778	29.9	101253.061	10.125	82
12:31AM	0.3	0.7	-0.4	78.3	25.72222222	29.9	101253.061	10.125	83
1:31AM	0.3	0.7	-0.4	78.6	25.88888889	29.9	101253.061	10.125	82
2:31AM	0.1	0.8	-0.7	79.3	26.27777778	29.8	100914.422	10.091	82
3:31AM	0.4	1.1	-0.7	79.7	26.5	29.8	100914.422	10.091	82
4:31AM	0.1	1.2	-1.1	80.1	26.72222222	29.8	100914.422	10.091	82
5:31AM	0.1	0.4	-0.3	80.4	26.88888889	29.8	100914.422	10.091	83
6:31AM	0.4	1	-0.6	80.4	26.88888889	29.8	100914.422	10.091	81
7:31AM	0.1	1.4	-1.3	80.4	26.88888889	29.8	100914.422	10.091	82
8:31AM	0.4	1	-0.6	80.6	27	29.8	100914.422	10.091	83

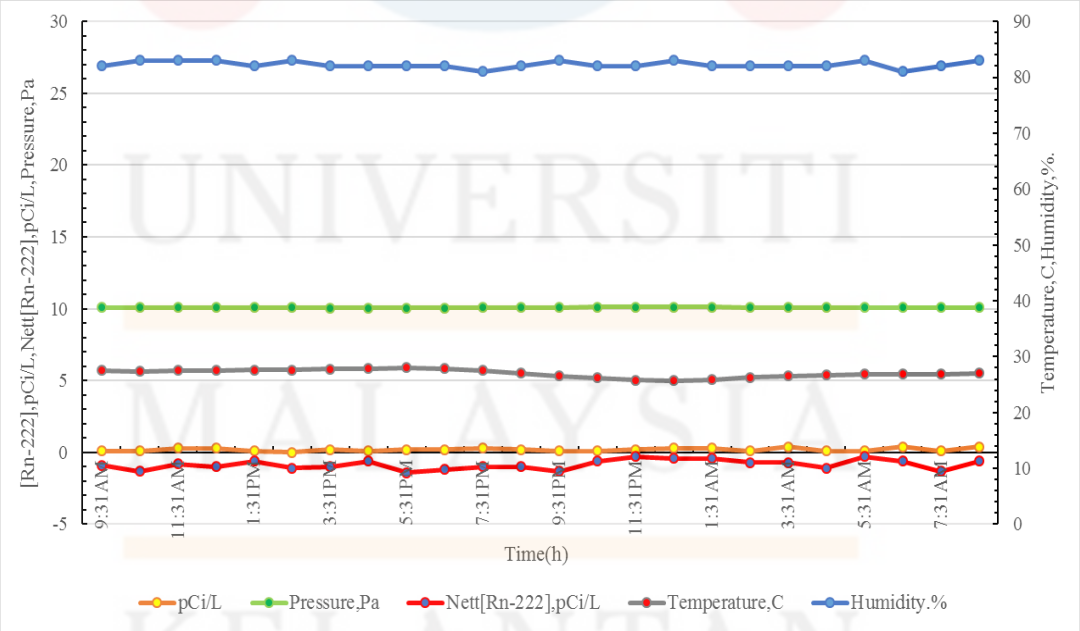

Figure B.4: Graph for second main data Rn-222 concentration in day 4

Table B.5: Data collected for second main data Rn-222 concentration in day 5

Date/Time	[Rn-222]	Background,	Nett,	Temperature,	Temperature,	Pressure,	Pressure,	Pressure,	Humidity
	pCi/l	pCi/L	pCi/L	F	˚C	inHg	Pa	Pax10^4	%
9:36AM	0.1	1	-0.9	80.4	26.88888889	29.8	100914.422	10.091	82
10:36AM	0.1	1.4	-1.3	80.2	26.77777778	29.9	101253.061	10.125	83
11:36AM	0.1	1.1	-1	80.4	26.88888889	29.8	100914.422	10.091	82
12:36PM	0.1	1.3	-1.2	80.6	27	29.8	100914.422	10.091	82
1:36PM	0.2	0.7	-0.5	80.8	27.11111111	29.8	100914.422	10.091	81
2:36:PM	0.2	1.1	-0.9	81	27.22222222	29.7	100575.783	10.058	82
3:36PM	0.1	1.2	-1.1	81.1	27.27777778	29.7	100575.783	10.058	81
4:36PM	0.1	0.7	-0.6	81.5	27.5	29.7	100575.783	10.058	82
5:36PM	0.2	1.6	-1.4	81.5	27.5	29.7	100575.783	10.058	82
6:36PM	0.3	1.4	-1.1	81	27.22222222	29.8	100914.422	10.091	82
7:36PM	0.3	1.3	-1	80.1	26.72222222	29.8	100914.422	10.091	82
8:36PM	0.2	1.2	-1	79.2	26.22222222	29.8	100914.422	10.091	81
9:36PM	0.2	1.4	-1.2	78.6	25.88888889	29.8	100914.422	10.091	82
10:36PM	0.2	0.7	-0.5	78.3	25.72222222	29.8	100914.422	10.091	83
11:36PM	0.2	0.5	-0.3	77.9	25.5	29.9	101253.061	10.125	83
12:36AM	0.2	0.7	-0.5	78.1	25.61111111	29.9	101253.061	10.125	83
1:36AM	0	0.7	-0.7	78.6	25.88888889	29.8	100914.422	10.091	82
2:36AM	0.1	0.8	-0.7	79	26.11111111	29.8	100914.422	10.091	82
3:36AM	0.4	1.1	-0.7	79.3	26.27777778	29.8	100914.422	10.091	82
4:36AM	0.1	1.2	-1.1	79.5	26.38888889	29.8	100914.422	10.091	83
5:36AM	0.2	0.4	-0.2	79.5	26.38888889	29.8	100914.422	10.091	82
6:36AM	0.2	1	-0.8	79.7	26.5	29.8	100914.422	10.091	82
7:36AM	0.2	1.4	-1.2	79.5	26.38888889	29.8	100914.422	10.091	81
8:36AM	0.4	1	-0.6	79.7	26.5	29.8	100914.422	10.091	83

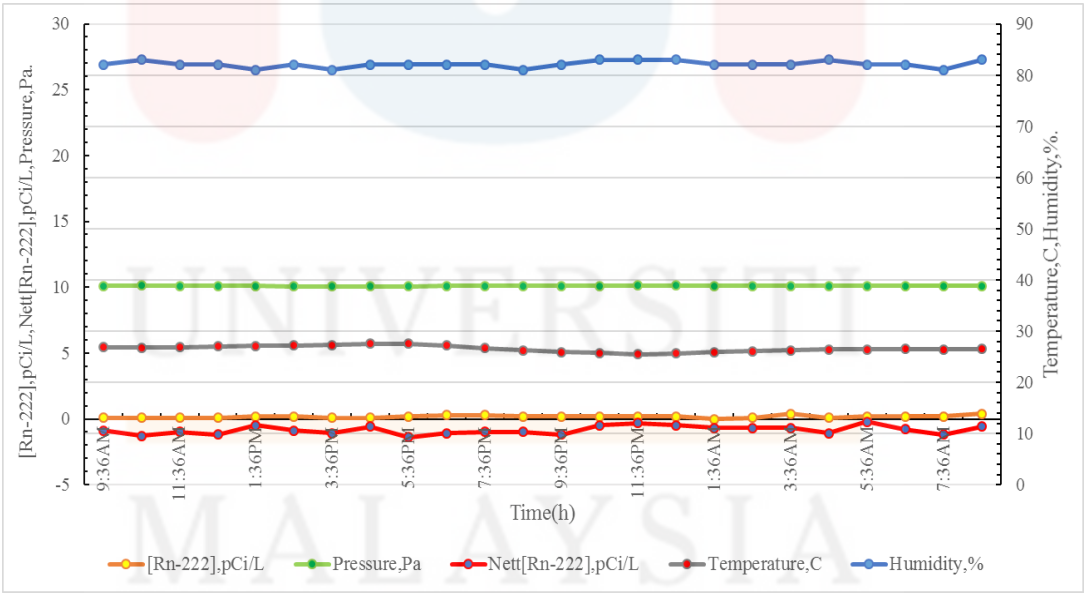

Figure B.5: Graph for second main data Rn-222 concentration in day 5

APPENDIX C

Table C.1: Data collected for third main data Rn-222 concentration in day 1

Date/Time	[Rn-222]	Background,	Nett,	Temperature,	Temperature,	Pressure,	Pressure,	Pressure,	Humidity
	pCi/l	pCi/L	pCi/L	F	˚C	inHg	Pa	Pax10^4	%
9:03AM	0.3	1	-0.7	79.2	26.22222222	29.9	101253.061	10.125	78
10:03AM	0.2	1.4	-1.2	79.5	26.38888889	29.9	101253.061	10.125	78
11:03AM	0.1	1.1	-1	80.1	26.72222222	29.9	101253.061	10.125	77
12:03PM	0.3	1.3	-1	80.8	27.11111111	29.9	101253.061	10.125	77
1:03PM	0.3	0.7	-0.4	81.5	27.5	29.8	100914.422	10.091	78
2:03PM	0.2	1.1	-0.9	82.4	28	29.8	100914.422	10.091	78
3:03PM	0.4	1.2	-0.8	83.1	28.38888889	29.8	100914.422	10.091	77
4:03PM	0.1	0.7	-0.6	83.3	28.5	29.8	100914.422	10.091	78
5:03PM	0.1	1.6	-1.5	83.3	28.5	29.8	100914.422	10.091	77
6:03PM	0.1	1.4	-1.3	83.1	28.38888889	29.8	100914.422	10.091	77
7:03PM	0.1	1.3	-1.2	82.9	28.27777778	29.8	100914.422	10.091	77
8:03PM	0.1	1.2	-1.1	82.8	28.22222222	29.9	101253.061	10.125	78
9:03PM	0.3	1.4	-1.1	82.6	28.11111111	29.9	101253.061	10.125	77
10:03PM	0.2	0.7	-0.5	82.4	28	29.9	101253.061	10.125	77
11:03PM	0.2	0.5	-0.3	82.2	27.88888889	29.9	101253.061	10.125	77
12:03AM	0.3	0.7	-0.4	82.2	27.88888889	29.9	101253.061	10.125	77
1:03AM	0.2	0.7	-0.5	82	27.77777778	29.9	101253.061	10.125	77
2:03AM	0.3	0.8	-0.5	81.9	27.72222222	29.9	101253.061	10.125	76
3:03AM	0.1	1.1	-1	81.7	27.61111111	29.9	101253.061	10.125	76
4:03AM	0.1	1.2	-1.1	81.7	27.61111111	29.9	101253.061	10.125	77
5:03AM	0.1	0.4	-0.3	81.5	27.5	29.9	101253.061	10.125	77
6:03AM	0.1	1	-0.9	81.5	27.5	29.9	101253.061	10.125	76
7:03AM	0.1	1.4	-1.3	81.3	27.38888889	29.9	101253.061	10.125	77
8:03AM	0.1	1	-0.9	81.3	27.38888889	29.9	101253.061	10.125	77

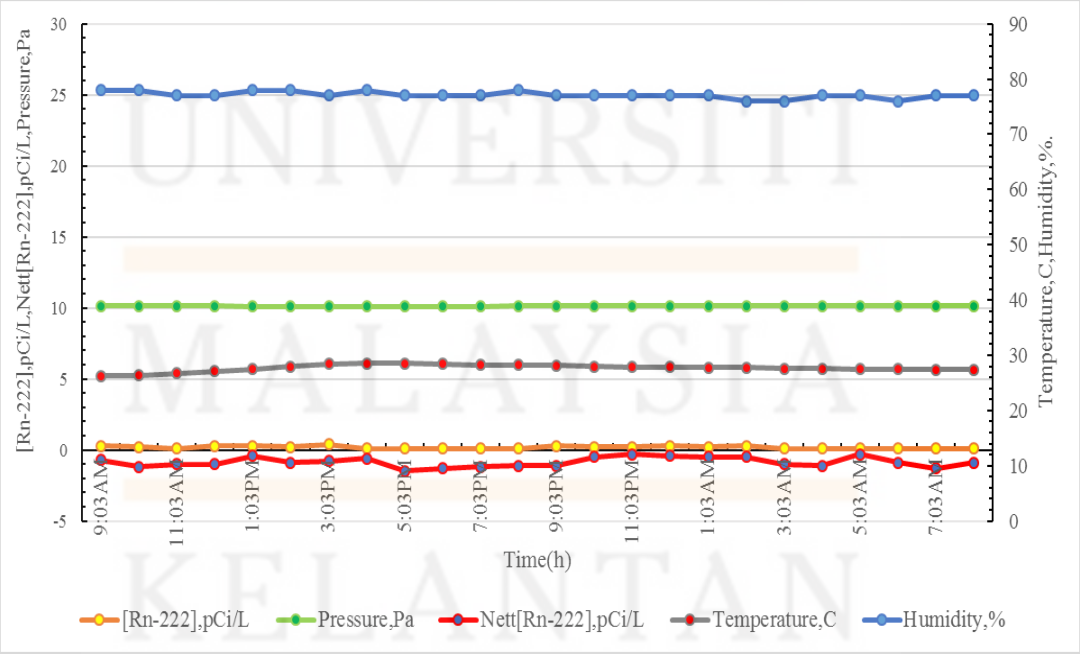

Figure C.1: Graph for third main data Rn-222 concentration in day 1

Table C.2: Data collected for third main data Rn-222 concentration in day 2

Date/Time	[Rn-222]	Background,	Nett,	Temperature,	Temperature,	Pressure,	Pressure,	Pressure,	Humidity,
	pCi/l	pCi/L	pCi/L	F	˚C	inHg	Pa	Pax10^4	%
9:22AM	0.3	1	-0.7	81.3	27.38888889	29.9	101253.061	10.125	76
10:22AM	0.2	1.4	-1.2	80.6	27	29.9	101253.061	10.125	76
11:22AM	0.2	1.1	-0.9	80.4	26.88888889	29.9	101253.061	10.125	76
12:22PM	0.2	1.3	-1.1	80.6	27	29.9	101253.061	10.125	77
1:22PM	0.5	0.7	-0.2	80.6	27	29.9	101253.061	10.125	75
2:22PM	0.4	1.1	-0.7	80.6	27	29.8	100914.422	10.091	76
3:22PM	0.5	1.2	-0.7	80.6	27	29.8	100914.422	10.091	76
4:22PM	0.4	0.7	-0.3	80.8	27.11111111	29.8	100914.422	10.091	75
5:22PM	0.1	1.6	-1.5	80.8	27.11111111	29.8	100914.422	10.091	76
6:22PM	0.4	1.4	-1	80.6	27	29.8	100914.422	10.091	75
7:22PM	0.5	1.3	-0.8	80.1	26.72222222	29.8	100914.422	10.091	76
8:22PM	0.5	1.2	-0.7	79.5	26.38888889	29.8	100914.422	10.091	75
9:22PM	0.2	1.4	-1.2	78.8	26	29.9	101253.061	10.125	75
10:22PM	0.6	0.7	-0.1	78.4	25.77777778	29.9	101253.061	10.125	76
11:22PM	0.2	0.5	-0.3	78.3	25.72222222	29.9	101253.061	10.125	76
12:22AM	0.2	0.7	-0.5	78.8	26	29.9	101253.061	10.125	75
1:22AM	0.4	0.7	-0.3	79.3	26.27777778	29.9	101253.061	10.125	75
2:22AM	0.5	0.8	-0.3	79.7	26.5	29.9	101253.061	10.125	75
3:22AM	0.4	1.1	-0.7	79.9	26.61111111	29.8	100914.422	10.091	75
4:22AM	0.4	1.2	-0.8	80.1	26.72222222	29.8	100914.422	10.091	74
5:22AM	0.5	0.4	0.1	80.2	26.77777778	29.8	100914.422	10.091	75
6:22AM	0.7	1	-0.3	80.2	26.77777778	29.8	100914.422	10.091	75
7:22AM	0.2	1.4	-1.2	80.2	26.77777778	29.9	101253.061	10.125	74
8:22AM	0.5	1	-0.5	80.2	26.77777778	29.9	101253.061	10.125	75

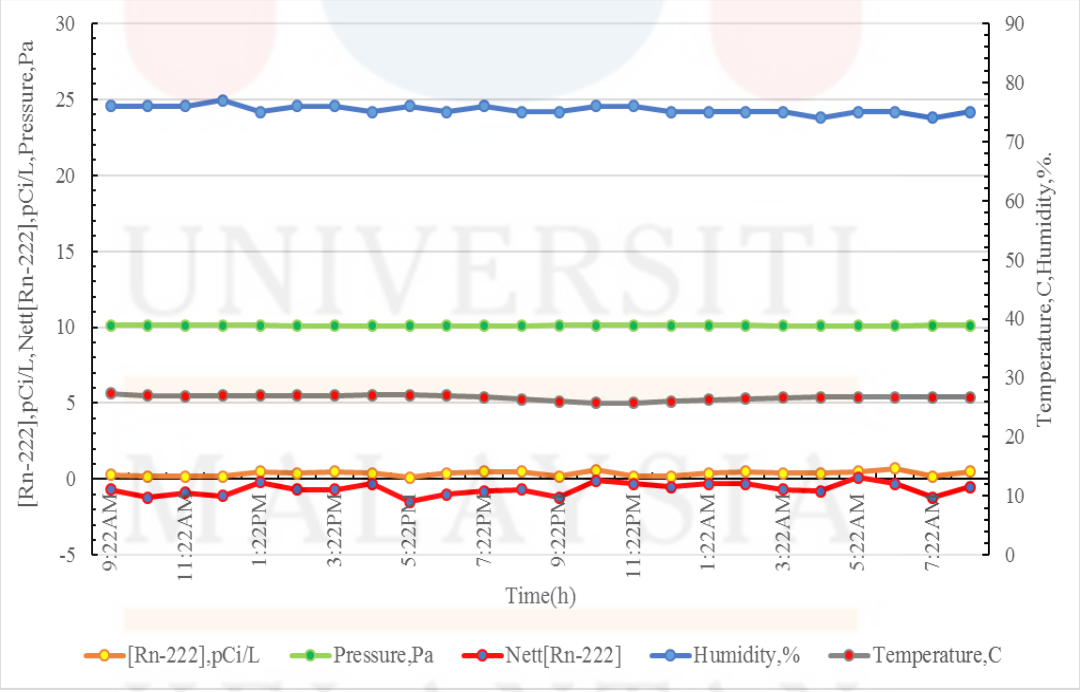

Figure C.2: Graph for third main data Rn-222 concentration in day 2

Table C.3: Data collected for third main data Rn-222 concentration in day 3

Date/Time	[Rn-222]	Background,	Nett,	Temperature,	Temperature,	Pressure,	Pressure	Pressure,	Humidity,
	pCi/l	pCi/L	pCi/L	F	˚C	inHg	,Pa	Pax10^4	%
9:27AM	0.4	1	-0.6	79.9	26.61111111	29.9	101253.061	10.125	75
10:27AM	0.4	1.4	-1	79.5	26.38888889	29.9	101253.061	10.125	75
11:27AM	0.4	1.1	-0.7	79.5	26.38888889	29.9	101253.061	10.125	76
12:27PM	0.5	1.3	-0.8	79.9	26.61111111	29.8	100914.422	10.091	75
1:27PM	0.6	0.7	-0.1	80.2	26.77777778	29.8	100914.422	10.091	75
2:27PM	0.3	1.1	-0.8	81	27.22222222	29.8	100914.422	10.091	74
3:27PM	0.4	1.2	-0.8	81.3	27.38888889	29.7	100575.783	10.058	74
4:27PM	0.3	0.7	-0.4	81.7	27.61111111	29.8	100914.422	10.091	74
5:27PM	0.4	1.6	-1.2	81.5	27.5	29.8	100914.422	10.091	75
6:27PM	0.4	1.4	-1	80.8	27.11111111	29.8	100914.422	10.091	75
7:27PM	0.4	1.3	-0.9	80.1	26.72222222	29.8	100914.422	10.091	74
8:27PM	0.6	1.2	-0.6	79.3	26.27777778	29.8	100914.422	10.091	75
9:27PM	0.5	1.4	-0.9	78.8	26	29.8	100914.422	10.091	75
10:27PM	0.2	0.7	-0.5	78.4	25.77777778	29.9	101253.061	10.125	74
11:27PM	0.3	0.5	-0.2	77.7	25.38888889	29.9	101253.061	10.125	74
12:27AM	0.7	0.7	0	77.9	25.5	29.9	101253.061	10.125	74
1:27AM	0.6	0.7	-0.1	78.6	25.88888889	29.8	100914.422	10.091	74
2:27AM	0.4	0.8	-0.4	79	26.11111111	29.8	100914.422	10.091	74
3:27AM	0.7	1.1	-0.4	79.2	26.22222222	29.8	100914.422	10.091	75
4:27AM	0.9	1.2	-0.3	79.3	26.27777778	29.8	100914.422	10.091	74
5:27AM	0.3	0.4	-0.1	79.3	26.27777778	29.8	100914.422	10.091	75
6:27AM	0.9	1	-0.1	79.3	26.27777778	29.8	100914.422	10.091	74
7:27AM	0.6	1.4	-0.8	79.3	26.27777778	29.8	100914.422	10.091	75
8:27AM	0.5	1	-0.5	79.5	26.38888889	29.9	101253.061	10.125	75

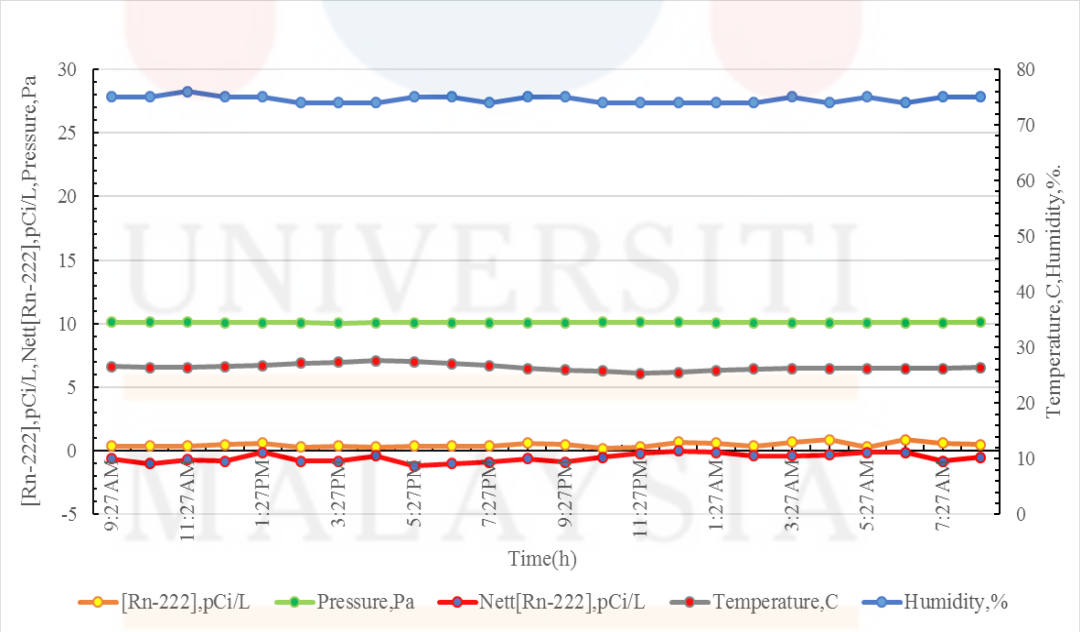

Figure C.3: Graph for third main data Rn-222 concentration in day 3

Table C.4: Data collected for third main data Rn-222 concentration in day 4

Date/Time	[Rn-222],	Background,	Nett,	Temperature,	Temperature,	Pressure,	Pressure,	Pressure,	Humidity,
	pCi/l	pCi/L	pCi/L	F	˚C	inHg	Pa	Pax10^4	%
9:35AM	1.2	1	0.2	79	26.11111111	29.9	101253.061	10.125	74
10:35AM	0.4	1.4	-1	78.6	25.88888889	29.9	101253.061	10.125	75
11:35AM	0.2	1.1	-0.9	79	26.11111111	29.8	100914.422	10.091	74
12:35PM	0.7	1.3	-0.6	79.3	26.27777778	29.8	100914.422	10.091	75
1:35PM	0.7	0.7	0	80.1	26.72222222	29.8	100914.422	10.091	74
2:35PM	0.8	1.1	-0.3	80.6	27	29.8	100914.422	10.091	74
3:35PM	0.7	1.2	-0.5	81.1	27.27777778	29.7	100575.783	10.058	74
4:35PM	0.4	0.7	-0.3	81.3	27.38888889	29.7	100575.783	10.058	74
5:35PM	0.7	1.6	-0.9	81.3	27.38888889	29.7	100575.783	10.058	74
6:35PM	1.1	1.4	-0.3	81.1	27.27777778	29.7	100575.783	10.058	73
7:35PM	0.7	1.3	-0.6	80.6	27	29.8	100914.422	10.091	74
8:35PM	0.4	1.2	-0.8	79.9	26.61111111	29.8	100914.422	10.091	75
9:35PM	0.4	1.4	-1	79.2	26.22222222	29.8	100914.422	10.091	74
10:35PM	0.5	0.7	-0.2	78.4	25.77777778	29.8	100914.422	10.091	75
11:35PM	0.5	0.5	0	77.7	25.38888889	29.8	100914.422	10.091	74
12:35AM	0.5	0.7	-0.2	77.2	25.11111111	29.8	100914.422	10.091	74
1:35AM	0.5	0.7	-0.2	76.8	24.88888889	29.8	100914.422	10.091	74
2:35AM	0.8	0.8	0	76.3	24.61111111	29.8	100914.422	10.091	75
3:35AM	0.3	1.1	-0.8	75.9	24.38888889	29.8	100914.422	10.091	74
4:35AM	0.3	1.2	-0.9	75.4	24.11111111	29.8	100914.422	10.091	74
5:35AM	0.8	0.4	0.4	75	23.88888889	29.8	100914.422	10.091	74
6:35AM	1.1	1	0.1	74.7	23.72222222	29.8	100914.422	10.091	74
7:35AM	0.8	1.4	-0.6	74.1	23.38888889	29.8	100914.422	10.091	74
8:35AM	0.6	1	-0.4	74.1	23.38888889	29.8	100914.422	10.091	73

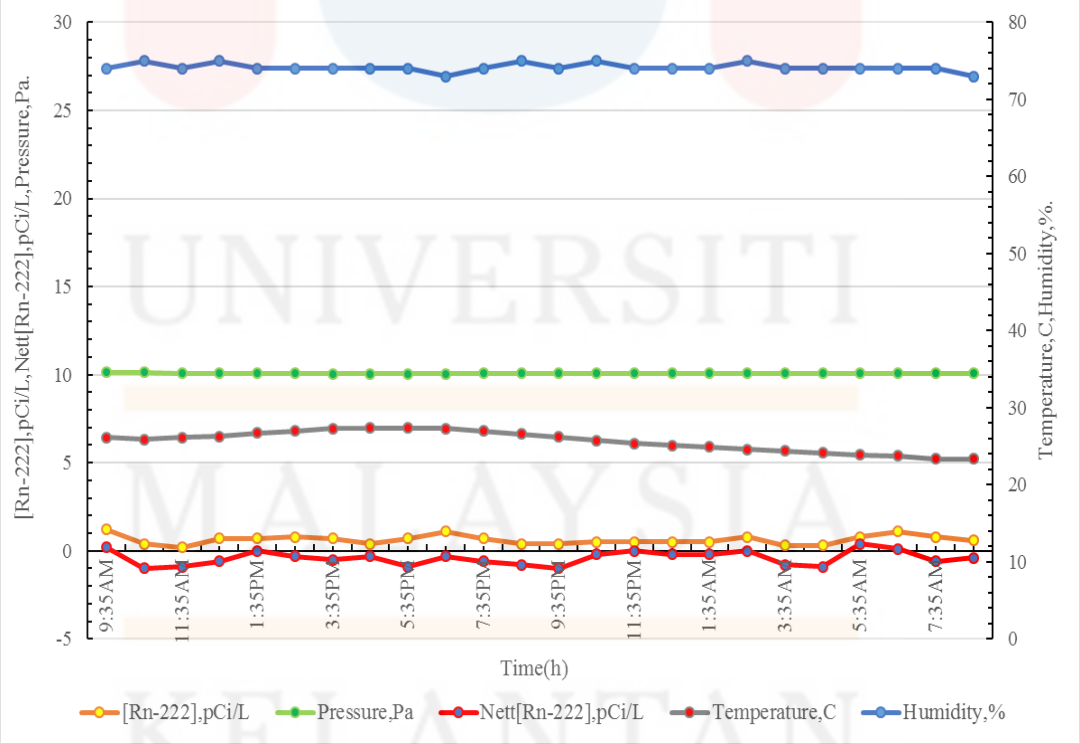

Figure C.4: Graph for third main data Rn-222 concentration in day 4

Table C.5: Data collected for third main data Rn-222 concentration in day 5

Date/Time	[Rn-222]	Background,	Nett,	Temperature,	Temperature,	Pressure,	Pressure,	Pressure,	Humidity,
	pCi/l	pCi/L	pCi/L	F	˚C	inHg	Pa	Pax10^4	%
9:41AM	0.5	1	-0.5	74.7	23.72222222	29.8	100914.422	10.091	74
10:41AM	0.8	1.4	-0.6	75.6	24.22222222	29.8	100914.422	10.091	74
11:41AM	0.7	1.1	-0.4	76.6	24.77777778	29.8	100914.422	10.091	73
12:41PM	0.6	1.3	-0.7	77.5	25.27777778	29.8	100914.422	10.091	74
1:41PM	0.5	0.7	-0.2	78.4	25.77777778	29.8	100914.422	10.091	73
2:41PM	0.7	1.1	-0.4	79.2	26.22222222	29.7	100575.783	10.058	73
3:41PM	1.2	1.2	0	79.5	26.38888889	29.7	100575.783	10.058	73
4:41PM	1	0.7	0.3	79.3	26.27777778	29.7	100575.783	10.058	73
5:41PM	0.7	1.6	-0.9	79	26.11111111	29.8	100914.422	10.091	73
6:41PM	0.6	1.4	-0.8	78.8	26	29.8	100914.422	10.091	73
7:41PM	0.5	1.3	-0.8	78.4	25.77777778	29.8	100914.422	10.091	73
8:41PM	0.8	1.2	-0.4	78.1	25.61111111	29.8	100914.422	10.091	73
9:41PM	0.8	1.4	-0.6	77.5	25.27777778	29.8	100914.422	10.091	73
10:41PM	0.8	0.7	0.1	77	25	29.8	100914.422	10.091	74
11:41PM	0.7	0.5	0.2	76.6	24.77777778	29.8	100914.422	10.091	74
12:41AM	1.1	0.7	0.4	77	25	29.8	100914.422	10.091	74
1:41AM	1.1	0.7	0.4	77.5	25.27777778	29.8	100914.422	10.091	74
2:41AM	0.7	0.8	-0.1	77.9	25.5	29.8	100914.422	10.091	74
3:41AM	0.9	1.1	-0.2	78.1	25.61111111	29.8	100914.422	10.091	73
4:41AM	0.5	1.2	-0.7	78.3	25.72222222	29.8	100914.422	10.091	73
5:41AM	0.5	0.4	0.1	78.3	25.72222222	29.8	100914.422	10.091	72
6:41AM	0.3	1	-0.7	78.3	25.72222222	29.8	100914.422	10.091	74
7:41AM	0.8	1.4	-0.6	78.3	25.72222222	29.8	100914.422	10.091	74
8:41AM	0.9	1	-0.1	78.6	25.88888889	29.8	100914.422	10.091	73

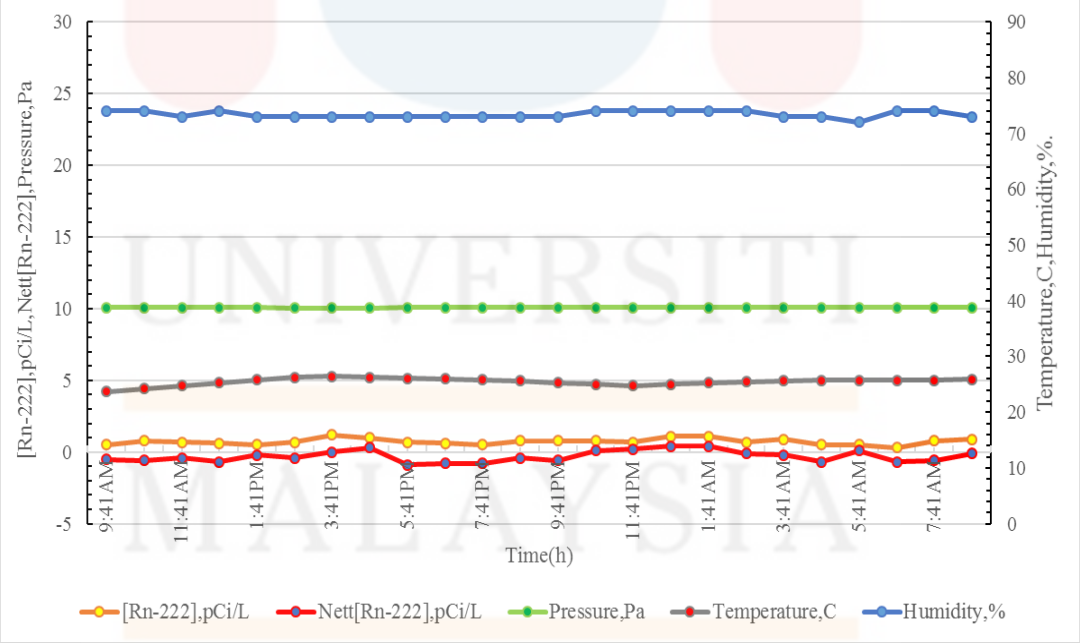

Figure C.5: Graph for third main data Rn-222 concentration in day 5

APPENDIX D

Table D.1: Data collected for fourth main data Rn-222 concentration in day 1

Date/Time	[Rn-222]	Background,	Nett,	Temperature,	Temperature,	Pressure,	Pressure,	Pressure,	Humidity
	pCi/L	pCi/L	pCi/L	F	˚C	inHg	Pa	Pax10^4	%
9:21AM	0.2	1	-0.8	75	23.88888889	29.8	100914.422	10.091	77
10:21AM	0.3	1.4	-1.1	76.1	24.5	29.8	100914.422	10.091	77
11:21AM	0.2	1.1	-0.9	77.2	25.11111111	29.8	100914.422	10.091	76
12:21PM	0.4	1.3	-0.9	78.4	25.77777778	29.8	100914.422	10.091	76
1:21PM	0.2	0.7	-0.5	79.5	26.38888889	29.8	100914.422	10.091	77
2:21PM	0.1	1.1	-1	80.6	27	29.7	100575.783	10.058	76
3:21PM	0.3	1.2	-0.9	81.7	27.61111111	29.7	100575.783	10.058	76
4:21PM	0.1	0.7	-0.6	82.8	28.22222222	29.7	100575.783	10.058	76
5:21PM	0.4	1.6	-1.2	83.7	28.72222222	29.7	100575.783	10.058	76
6:21PM	0.3	1.4	-1.1	84.2	29	29.7	100575.783	10.058	76
7:21PM	0.1	1.3	-1.2	84.6	29.22222222	29.7	100575.783	10.058	77
8:21PM	0.1	1.2	-1.1	84.6	29.22222222	29.8	100914.422	10.091	76
9:21PM	0.1	1.4	-1.3	84.6	29.22222222	29.8	100914.422	10.091	77
10:21PM	0.1	0.7	-0.6	84.4	29.11111111	29.8	100914.422	10.091	76
11:21PM	0.2	0.5	-0.3	84.2	29	29.8	100914.422	10.091	76
12:21AM	0.2	0.7	-0.5	84	28.88888889	29.8	100914.422	10.091	76
1:21AM	0.4	0.7	-0.3	83.7	28.72222222	29.8	100914.422	10.091	77
2:21AM	0.2	0.8	-0.6	83.3	28.5	29.8	100914.422	10.091	77
3:21AM	0	1.1	-1.1	83.1	28.38888889	29.8	100914.422	10.091	77
4:21AM	0.2	1.2	-1	82.9	28.27777778	29.8	100914.422	10.091	78
5:21AM	0.7	0.4	0.3	82.6	28.11111111	29.8	100914.422	10.091	78
6:21AM	0.2	1	-0.8	82.4	28	29.8	100914.422	10.091	78
7:21AM	0.5	1.4	-0.9	82.2	27.88888889	29.8	100914.422	10.091	77
8:21AM	0.1	1	-0.9	82.2	27.88888889	29.8	100914.422	10.091	76

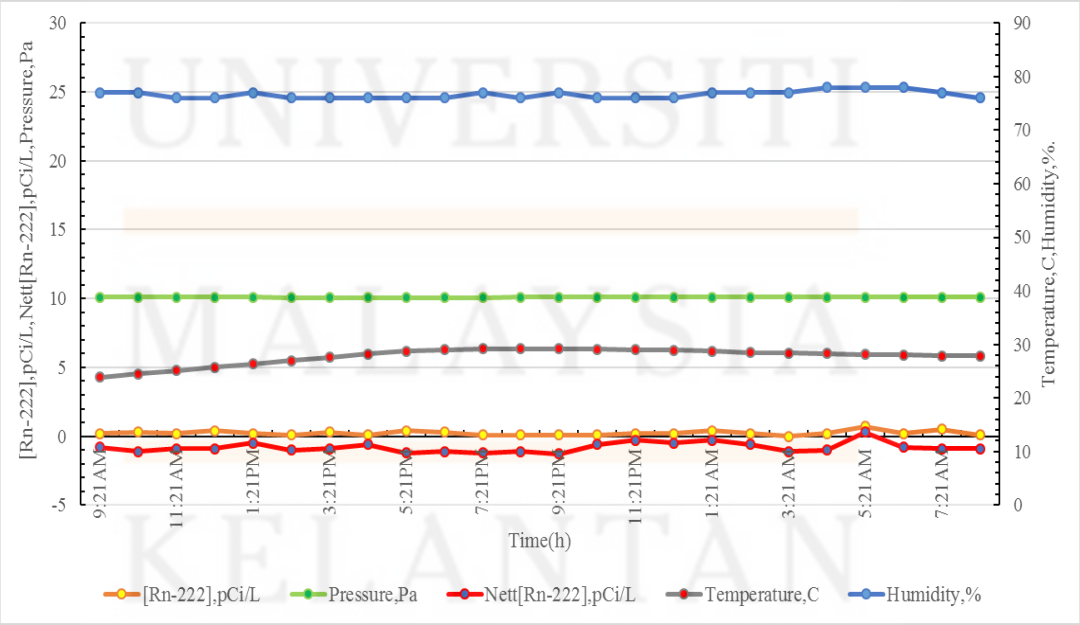

Figure D.1: Graph for fourth main data Rn-222 concentration in day 1

Table D.2: Data collected for fourth main data Rn-222 concentration in day 2

Date/Time	[Rn-222] pCi/l	Background, pCi/L	Nett, pCi/L	Temperature, F	Temperature, ˚C	Pressure, inHg	Pressure, Pa	Pressure ,Pax10^4	Humidity, %
9:26AM	0.2	1	-0.8	82.6	28.11111111	29.8	100914.422	10.091	77
10:26AM	0.2	1.4	-1.2	83.1	28.38888889	29.8	100914.422	10.091	78
11:26AM	0.2	1.1	-0.9	83.7	28.72222222	29.8	100914.422	10.091	77
12:26PM	0.2	1.3	-1.1	84.4	29.11111111	29.8	100914.422	10.091	77
1:26PM	0.2	0.7	-0.5	84.9	29.38888889	29.8	100914.422	10.091	76
2:26PM	0.1	1.1	-1	85.5	29.72222222	29.8	100914.422	10.091	77
3:26PM	0.2	1.2	-1	86	30	29.7	100575.783	10.058	78
4:26PM	0.4	0.7	-0.3	86.7	30.38888889	29.7	100575.783	10.058	76
5:26PM	0.2	1.6	-1.4	87.4	30.77777778	29.7	100575.783	10.058	77
6:26PM	0.1	1.4	-1.3	87.8	31	29.7	100575.783	10.058	77
7:26PM	0.2	1.3	-1.1	88	31.11111111	29.7	100575.783	10.058	77
8:26PM	0.3	1.2	-0.9	87.8	31	29.8	100914.422	10.091	76
9:26PM	0.3	1.4	-1.1	87.6	30.88888889	29.8	100914.422	10.091	76
10:26PM	0.2	0.7	-0.5	87.3	30.72222222	29.8	100914.422	10.091	77
11:26PM	0.2	0.5	-0.3	86.9	30.5	29.8	100914.422	10.091	78
12:26AM	0.1	0.7	-0.6	86.5	30.27777778	29.8	100914.422	10.091	77
1:26AM	0.4	0.7	-0.3	86.4	30.22222222	29.8	100914.422	10.091	78
2:26AM	0.2	0.8	-0.6	86	30	29.8	100914.422	10.091	78
3:26AM	0.1	1.1	-1	85.8	29.88888889	29.8	100914.422	10.091	78
4:26AM	0.2	1.2	-1	85.5	29.72222222	29.8	100914.422	10.091	77
5:26AM	0.2	0.4	-0.2	85.3	29.61111111	29.8	100914.422	10.091	76
6:26AM	0.1	1	-0.9	84.9	29.38888889	29.8	100914.422	10.091	77
7:26AM	0.3	1.4	-1.1	84.7	29.27777778	29.8	100914.422	10.091	78
8:26AM	0.4	1	-0.6	84.6	29.22222222	29.8	100914.422	10.091	77

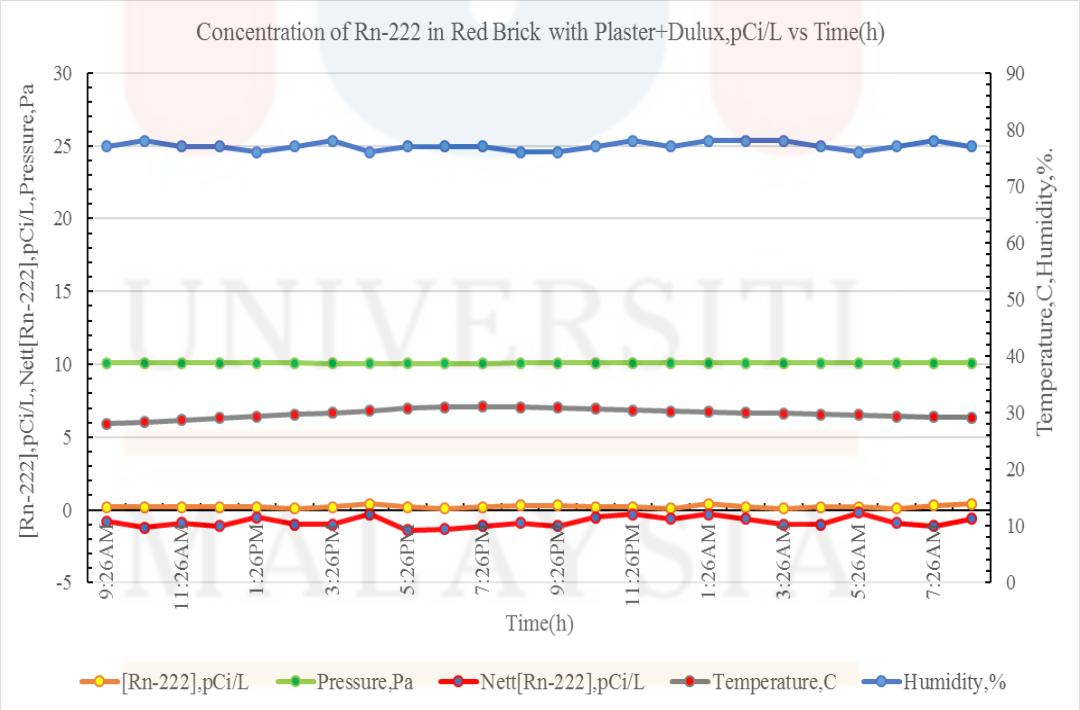

Figure D.2: Graph for fourth main data Rn-222 concentration in day 2

Table D.3: Data collected for fourth main data Rn-222 concentration in day 3

Date/Time	[Rn-222]	Background,	Nett,	Temperature,	Temperature,	Pressure,	Pressure,	Pressure,	Humidity
	pCi/l	pCi/L	pCi/L	F	˚C	inHg	Pa	Pax10^4	%
9:33AM	0.1	1	-0.9	83.7	28.72222222	29.9	101253.061	10.125	78
10:33AM	0.3	1.4	-1.1	82.8	28.22222222	29.9	101253.061	10.125	78
11:33AM	0.4	1.1	-0.7	82.6	28.11111111	29.8	100914.422	10.091	78
12:33PM	0.2	1.3	-1.1	82.6	28.11111111	29.8	100914.422	10.091	78
1:33PM	0.2	0.7	-0.5	82.8	28.22222222	29.8	100914.422	10.091	78
2:33PM	0.2	1.1	-0.9	82.9	28.27777778	29.8	100914.422	10.091	78
3:33PM	0.4	1.2	-0.8	83.1	28.38888889	29.7	100575.783	10.058	77
4:33PM	0.2	0.7	-0.5	83.3	28.5	29.7	100575.783	10.058	77
5:33PM	0.2	1.6	-1.4	83.5	28.61111111	29.7	100575.783	10.058	78
6:33PM	0.2	1.4	-1.2	83.3	28.5	29.7	100575.783	10.058	78
7:33PM	0.3	1.3	-1	82.9	28.27777778	29.8	100914.422	10.091	77
8:33PM	0.1	1.2	-1.1	82.4	28	29.8	100914.422	10.091	78
9:33PM	0.5	1.4	-0.9	81.7	27.61111111	29.8	100914.422	10.091	77
10:33PM	0.5	0.7	-0.2	80.8	27.11111111	29.8	100914.422	10.091	77
11:33PM	0.4	0.5	-0.1	80.1	26.72222222	29.8	100914.422	10.091	78
12:33AM	0.2	0.7	-0.5	80.1	26.72222222	29.8	100914.422	10.091	78
1:33AM	0.1	0.7	-0.6	80.8	27.11111111	29.8	100914.422	10.091	77
12:33AM	0.1	0.8	-0.7	81.5	27.5	29.8	100914.422	10.091	77
3:33AM	0.2	1.1	-0.9	82	27.77777778	29.8	100914.422	10.091	76
4:33AM	0.2	1.2	-1	82.4	28	29.8	100914.422	10.091	77
5:33AM	0.4	0.4	0	82.8	28.22222222	29.7	100575.783	10.058	78
6:33AM	0.2	1	-0.8	82.8	28.22222222	29.8	100914.422	10.091	77
7:33AM	0.1	1.4	-1.3	82.9	28.27777778	29.8	100914.422	10.091	78
8:33AM	0.3	1	-0.7	82.9	28.27777778	29.8	100914.422	10.091	77

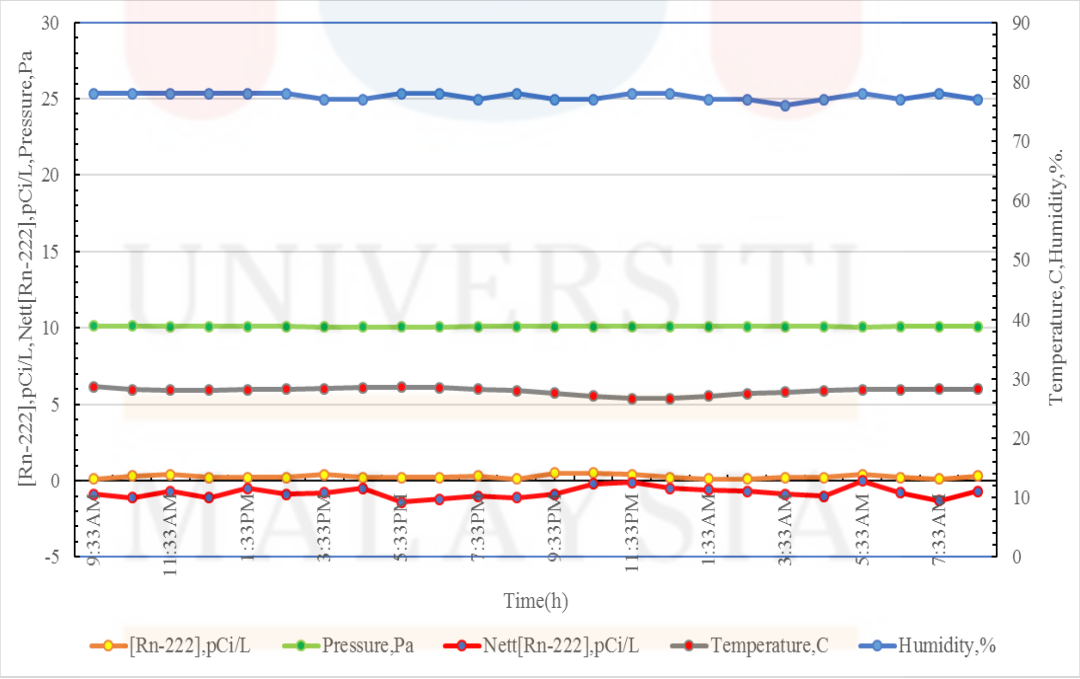

Figure D.3: Graph for fourth main data Rn-222 concentration in day 3

Table D.4: Data collected for fourth main data Rn-222 concentration in day 4

Date/Time	[Rn-222]	Background,	Nett,	Temperature,	Temperature,	Pressure,	Pressure,	Pressure,	Humidity,
	pCi/l	pCi/L	pCi/L	F	˚C	inHg	Pa	Pax10^4	%
9:38AM	0.3	1	-0.7	82.4	28	29.8	100914.422	10.091	78
10:38AM	0.3	1.4	-1.1	81.7	27.61111111	29.8	100914.422	10.091	78
11:38AM	0.3	1.1	-0.8	81.3	27.38888889	29.8	100914.422	10.091	78
12:38PM	0.2	1.3	-1.1	81.5	27.5	29.8	100914.422	10.091	77
1:38PM	0.2	0.7	-0.5	81.7	27.61111111	29.8	100914.422	10.091	78
2:38PM	0.4	1.1	-0.7	82	27.77777778	29.7	100575.783	10.058	77
3:38PM	0.4	1.2	-0.8	82.4	28	29.7	100575.783	10.058	78
4:38PM	0.5	0.7	-0.2	82.8	28.22222222	29.7	100575.783	10.058	77
5:38PM	0.4	1.6	-1.2	82.6	28.11111111	29.7	100575.783	10.058	77
6:38PM	0.4	1.4	-1	82	27.77777778	29.7	100575.783	10.058	77
7:38PM	0.1	1.3	-1.2	81.1	27.27777778	29.8	100914.422	10.091	78
8:38PM	0.2	1.2	-1	80.4	26.88888889	29.8	100914.422	10.091	78
9:38PM	0.2	1.4	-1.2	79.9	26.61111111	29.8	100914.422	10.091	78
10:38PM	0.5	0.7	-0.2	79.2	26.22222222	29.8	100914.422	10.091	78
11:38PM	0.3	0.5	-0.2	78.6	25.88888889	29.8	100914.422	10.091	78
12:38AM	0.4	0.7	-0.3	78.8	26	29.8	100914.422	10.091	78
1:38AM	0.5	0.7	-0.2	79.5	26.38888889	29.8	100914.422	10.091	78
2:38AM	0.5	0.8	-0.3	80.1	26.72222222	29.8	100914.422	10.091	78
3:38AM	0.4	1.1	-0.7	80.4	26.88888889	29.8	100914.422	10.091	78
4:38AM	0.3	1.2	-0.9	80.6	27	29.8	100914.422	10.091	78
5:38AM	0.2	0.4	-0.2	80.8	27.11111111	29.8	100914.422	10.091	77
6:38AM	0.4	1	-0.6	81	27.22222222	29.8	100914.422	10.091	78
7:38AM	0.2	1.4	-1.2	81	27.22222222	29.8	100914.422	10.091	78
8:38AM	0.1	1	-0.9	81.1	27.27777778	29.8	100914.422	10.091	77

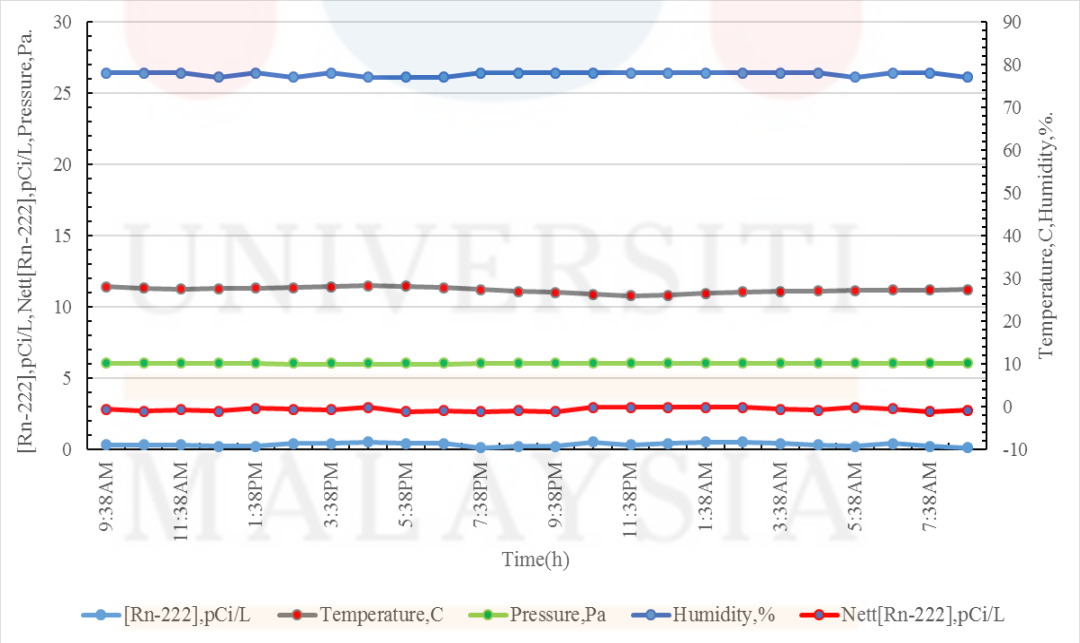

Figure D.4: Graph for fourth main data Rn-222 concentration in day 4

Table D.5: Data collected for fourth main data Rn-222 concentration in day 5

Date/Time	[Rn-222]	Background,	Nett,	Temperature,	Temperature,	Pressure,	Pressure,	Pressure,	Humidity,
	pCi/l	pCi/L	pCi/L	F	˚C	inHg	Pa	Pax10^4	%
9:41AM	0.1	1	-0.9	80.6	27	29.8	100914.422	10.091	78
10:41AM	0.3	1.4	-1.1	79.9	26.61111111	29.8	100914.422	10.091	77
11:41AM	0.4	1.1	-0.7	79.5	26.38888889	29.8	100914.422	10.091	77
12:41PM	0.5	1.3	-0.8	79.3	26.27777778	29.8	100914.422	10.091	78
1:41PM	0.1	0.7	-0.6	79.3	26.27777778	29.8	100914.422	10.091	78
12:41PM	0.2	1.1	-0.9	79.3	26.27777778	29.7	100575.783	10.058	78
3:41PM	0.3	1.2	-0.9	79.5	26.38888889	29.7	100575.783	10.058	77
4:41PM	0.2	0.7	-0.5	79.5	26.38888889	29.7	100575.783	10.058	77
5:41PM	0.3	1.6	-1.3	79.7	26.5	29.7	100575.783	10.058	77
6:41PM	0.2	1.4	-1.2	79.3	26.27777778	29.7	100575.783	10.058	77
7:41PM	0.2	1.3	-1.1	78.8	26	29.8	100914.422	10.091	78
8:41PM	0.1	1.2	-1.1	78.3	25.72222222	29.8	100914.422	10.091	79
9:41PM	0.4	1.4	-1	77.7	25.38888889	29.8	100914.422	10.091	77
10:41PM	0.4	0.7	-0.3	77.2	25.11111111	29.8	100914.422	10.091	79
11:41PM	0.4	0.5	-0.1	77.4	25.22222222	29.8	100914.422	10.091	78
12:41AM	0.2	0.7	-0.5	77.9	25.5	29.8	100914.422	10.091	77
1:41AM	0.5	0.7	-0.2	78.4	25.77777778	29.8	100914.422	10.091	78
2:41AM	0.4	0.8	-0.4	79	26.11111111	29.8	100914.422	10.091	77
3:41AM	0.4	1.1	-0.7	79.3	26.27777778	29.8	100914.422	10.091	78
4:41AM	0.1	1.2	-1.1	79.5	26.38888889	29.8	100914.422	10.091	77
5:41AM	0.1	0.4	-0.3	79.7	26.5	29.8	100914.422	10.091	78
6:41AM	0.3	1	-0.7	79.7	26.5	29.8	100914.422	10.091	78
7:41AM	0.5	1.4	-0.9	79.7	26.5	29.8	100914.422	10.091	76
8:41AM	0.3	1	-0.7	79.9	26.61111111	29.8	100914.422	10.091	78

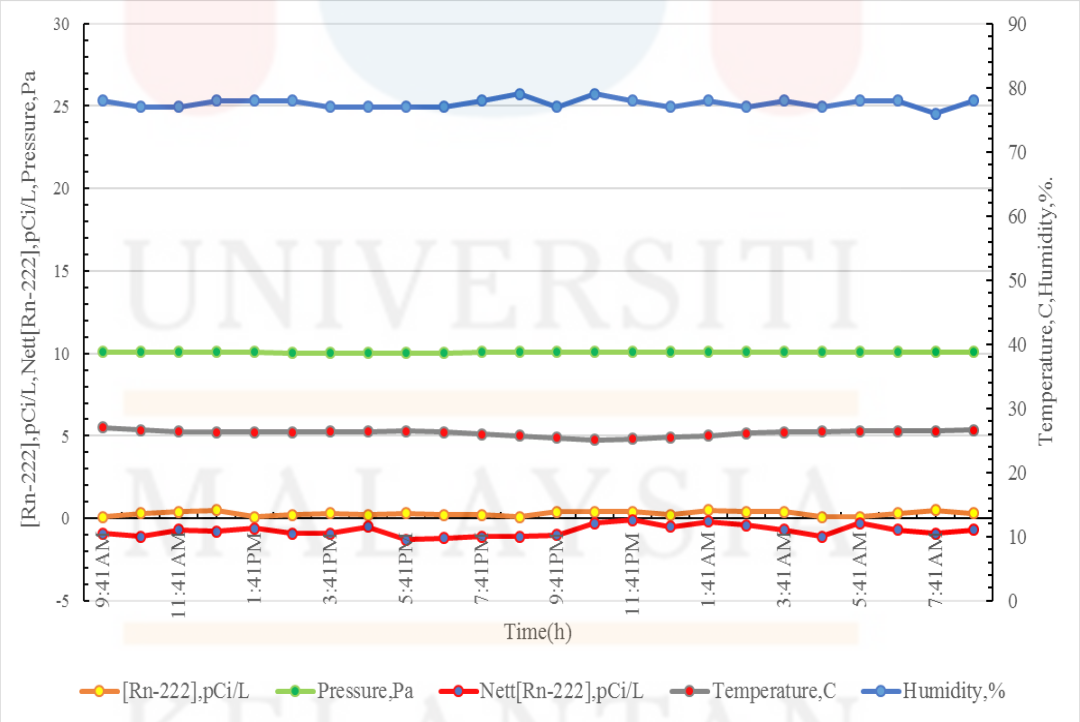

Figure D.5: Graph for fourth main data Rn-222 concentration in day 5

Table D.6: Specification of Radon Sentinel 1030

Features	Specifications
Interval settings	Delay selection(hr): 0,12,24,48 Duration selection (hr): 1,12, 24, 36, 48, 60, 72, 84, 96, 100 or long test.
Sensitivity	15 cph per pCi/L
Measurement ranges	0.1 to 9999 pCi/L or; 1Bq/m^3 to 99.99 kBq/m^3
Measurement intervals	0.5, 1, 2, 4, 8, 12, 16, 20, 24 hours.
Humidity detector	Range: 20-95% Accuracy: ±5% Resolution: 1%
Temperature detector	Range: 45˚F to 95˚F (7˚C to 35˚C) Accuracy: 2˚F (1˚F)
Pressure detector.	Range: 2v0.4 – 30.5 in Hg (69-103 kPa) Accuracy: 1.0 in Hg (3.4 kPa) Resolution: 0.04 in Hg (0.14 kPa)
Disturbance detector	Reports shows “M” for motion.